UNIVERSIDADE D
COIMBRA

Beatriz Campos Raposo Medeiros Araújo

Drowsiness Detection Using a Headband and Artificial Neural Networks

Dissertation submitted to the University of Coimbra for the degree of Master in Biomedical Engineering, supervised by Prof. Dr. Mateus Mendes (IPC/ISR), Prof. Dr. Paulo Coimbra (DEEC-UC/ISR) and Prof. Dr. Manuel Crisóstomo (DEEC-UC/ISR).

September 2019

FACULDADE DE CIÊNCIAS E TECNOLOGIA
UNIVERSIDADE D COIMBRA

Beatriz Campos Raposo Medeiros Araújo

Drowsiness Detection Using a Headband and Artificial Neural Networks

Dissertation submitted to the
University of Coimbra for the degree of
Master in Biomedical Engineering

Supervisors:
Prof. Dr. Mateus Mendes (IPC/ISR)
Prof. Dr. Paulo Coimbra (DEEC-UC/ISR)
Prof. Dr. Manuel Crisóstomo (DEEC-UC/ISR)

Setembro, 2019

This work was developped in collaboration with:

"It is never too late to be what you might have been."

George Eliot

Acknowledgments

This dissertation wouldn't have been possible without the care and support from the people surrounding me over this years. For that, I want to express my gratitude towards them.

Thank you to my supervisors Prof. Dr. Mateus Mendes, Prof. Dr. Paulo Coimbra and Prof. Dr. Manuel Crisóstomo for all the guidance, assistance and lighthearted meetings throughout the year.

Also, an immense thank you to my family for all the care and support during this five years. Even far from home they were always present in my day to day life, encouraging me to overcome all the challenges along the way.

To Coimbra and all the friends I made here, a special thank you. This five years wouldn't have been possible without all the laughs, adventures and moments that we passed here together. Coimbra became a second home to me thanks to them.

To my friends from home and overseas an enormous thank you for all the patience and care. Even distant they were always there to confort me and to make me believe that the seemed impossible was possible.

Eternally greateful!

Resumo

Ao longo dos anos, a percentagem de população com carta de condução tem crescido rapidamente e, consequentemente, também a taxa de acidentes de viação. Sonolência é uma das principais razões para acidentes rodoviários por provocar um decréscimo de percepção, concentração e controlo sobre o veículo. Por esta razão, novas técnicas para prevenção de acidentes causados devido ao cansaço do condutor têm sido exploradas como, por exemplo, a possibilidade de prever se o condutor está sonolento ou não.

Este projeto tem como objetivo implementar técnicas de machine learning para identificação de diferentes estados mentais do condutor recorrendo ao uso de uma headband de fácil utilização e transporte, capaz de recolher ondas cerebrais. O estado mental do sujeito, neste caso de alerta ou sonolência, está diretamente interligado com a maior ou menor presença de certas frequências cerebrais, o que permite identificar em que condição o indivíduo se encontra. Para este fim, foram realizadas aquisições da atividade cerebral em distintas situações. Posteriormente, diversos métodos de identificação e remoção de ruído (artefatos) e algoritmos de séries temporais foram aplicados para a construção de datasets que, mais tarde, seriam classificados por uma rede neuronal com o objetivo de diferenciar entre estados de vigília e cansaço.

Palavras-chave - EEG, ICC, Headband para leitura de ondas cerebrais, Redes Neuronais Artificiais, Análise de séries temporais, Sonolência, Alerta

Abstract

Over the last years, the percentage of licensed drivers has increased rapidly and, as a consequence, so have car accidents. Drowsiness is one of the main reasons for car crashes due to a decrease of perception, concentration and control over the vehicle. For that reason, new techniques for prevention of accidents caused by somnolence have been explored. That includes, for example, prediction of non-alert states.

This project aims at implementing machine learning techniques for the identification of different mental states of the driver, with the use of a wearable and lightweight headband, capable of collecting brain signals. The mental state of the subject, in this case of alertness or somnolence, is directly interconnected with a higher or lower presence of certain brain frequencies that will enable to identify in which condition the individual is in. For that purpose, recordings of brain response to different scenarios, both in alert and drowsiness situations, were made. Different methods were applied to detect and reject noise (namely so called artifacts) and different time series algorithms were applied for the construction of datasets that were after be fed to an artificial neural network with the goal of differentiate between states of vigilance and drowsiness.

Keywords - EEG, BCI, Wearable brain sensing headband, Artificial Neural Networks, Time Series Analysis, Drowsiness, Alertness

Acronyms

ANN - Artificial Neural Network

BCI - Brain Computer Interface

BLE - Bluetooth Low-Energy

DRL - Driven Right Leg electrode

DWT - Discrete Wavelet Transform

EEG - Electroencephalography

EMG - Electromyography

EOG - Electrooculography

FFT - Fast Fourier Transform

fMRI - functional Magnetic Resonance Imaging

ICA - Independent Component Analysis

LDA - Linear Discriminant Analysis

PSD - Power Spectral Density

REF - Reference electrode

SCP - Slow Cortical Potential

SSVEP - Steady State Visually Evoked Potential

SVM - Support-Vector Machine

VEP - Visually Evoked Potential

List of Figures

List of Tables

Contents

1

Introduction

A study[1], from the Portuguese Pneumology Society, concluded that around 20% of the car accidents in Portugal are due to drowsiness of the driver. The same paper also claims that the risk of accident increases when driving longer distances and when the driver suffers from obstructive sleep apnea. Also, in the field of work safety, according to the Authority for Work Conditions, fatigue is one of the main causes for work accidents, mainly on the transports sector[2]. These are due to the fact that somnolence causes a decrease of brain activity that, as a consequence, will affect the person's behavior resulting in frequent yawning and blinking eyes, difficulty in focusing, slowing down, rambling thoughts and bad memory[1].

Numerous researches have been done with the goal of detecting the subject's level of alertness. Therefore, diverse physiological factors were taken into account, for the differentiation between an alert and a drowsy state such as, heart and pulse rate, eye blinking frequency and skin electric potential [1]. Despite all the different somnolence indicators, the direct measurement of brain activity, generated by the exchange of information between neurons and electro-chemical transmitters, has shown to be one of the most reliable [2][3].

Brain activity can be monitored by electrophysiological methods, such as electroencephalography (EEG) where weak electrical signals detected by electrodes positioned on the scalp are considerably amplified and stored to computer memory or printed in paper [2][4]. The measurement of EEG signals is a non-invasive procedure that is often known to have a large quantity of electrodes for a greater precision. However, there has been increasing research in the field of wearable and wireless EEG devices with as few as four channels [5]. Those systems have shown to be useful in cases where medical grade devices are impractical such as for drowsy drivers, where there is a need for a lightweight system. On the other hand, those simple headsets present

[1] SPP lança campanha "Não conduza de olhos fechados" published in 2017-08-04, http://www.sppneumologia.pt/noticias/noticia/spp-lana-campanha-no-conduza-de-olhos-fechados-04082017, visited in 2019-01-16

[2] Lusíadas -"Acidentes de trabalho: não corra risco", https://rotasaude.lusiadas.pt/acidentes-de-trabalho-nao-corra-riscos/, visited in 2019-03-05

a lack of resolution in comparison with more complex ones [6].

The goal of the present project is the possibility of differentiation between mental states, in this case drowsiness and alertness, using the MUSE brain sensing headset, manufactured by Interaxon Inc., with only four electrodes capable of reading EEG signals, two of them positioned between the pre-frontal and frontal regions (AF7 and AF8) and the other pair between the temporal and parietal lobes (TP9 and TP10). Data from the sensors are collected, processed and fed to a machine learning algorithm (artificial neural networks), for data classification [7].

For a detailed analysis of the topic, the present dissertation is divided in different chapters. In the Chapter 2, Brain Computer Interfaces, electroencephalography and the various frequency rhythms from the different regions of the brain are reviewed. In Chapter 3, past research in the field of drowsiness detection with EEG devices is explored. In the Chapter 4, the hardware and software used for the recording of the EEG signal and its analysis is described. In Chapter 5, the various methods used for artifacts removal, time series analysis and dataset and artificial neural network construction are explained. In Chapter 6, the obtained results are presented and examined. Finally, in Chapter 7 some conclusions and future work are highlighted.

2

BCI and Brain Waves

Nowadays, with the advance of technologies, it's possible to read electrical signals from the brain, which are mainly produced by neuronal postsynaptic membrane polarity changes as a result of the activation of voltage-gated or ion-gated channels [8]. In this chapter, the devices and methods for brain activity monitoring and interpretation will be described.

2.1 BCI System

The acquisition, analysis and translation of the electrical brain signals are done using devices called brain-computer interfaces (BCI) [8].

A BCI is a hardware and software communications system that can recognize a certain set of patterns in the signals of the brain depending on the output aimed by the user [2][8]. This system uses electroencephalographic or cortical single-neuron activity to control cursor movement, select letters or icons, or operate neuroprostheses through the transmission of brain signals to the muscles or to external prosthetic devices [9][10].

2.1.1 BCI Elements

For a successful use, a brain-computer system needs to have elements that will allow the signal acquisition, feature extraction, classification, and the control interface (Fig. 2.1) [2]. The usual steps performed by the BCI system are described bellow

Acquisition

During this stage, sensors are used to capture brain signals that will have to be amplified enough for the next stage of digital processing. Those signals may be

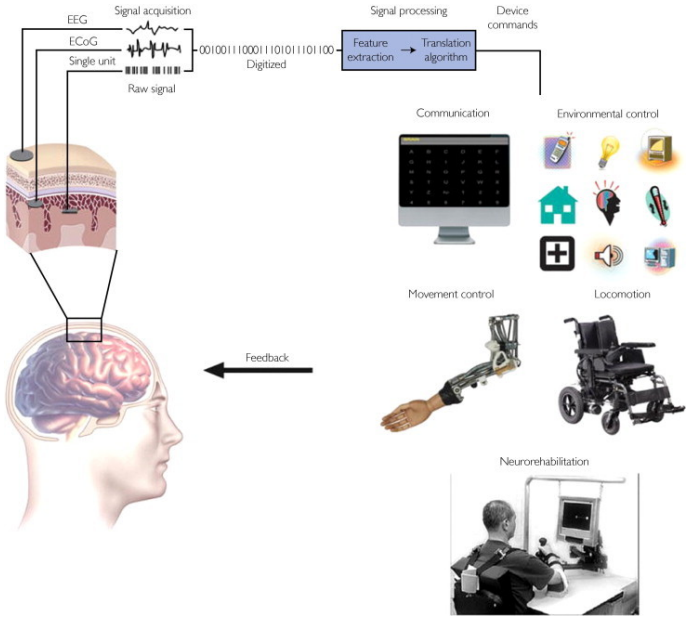

Figure 2.1: Components of a brain-compurter interface system [8].

subjected to filtering for noise reduction and artifact processing. One example of a sensor that can be used during this step is electrodes. Electrodes are required to study the electrophysiologic activity.

At the end of the acquisition stage, the resulting signals are read and transmitted to a computer [8].

Feature extraction

Since the brain activity results in different signals, and some overlap in both time and space, it is fundamental the analysis of the digital signals for identification of important information [2][8]. Signal contamination by unwanted noise results in diverse artifacts, that may be caused by the measurement equipment or by the test subject itself, will need to be filtered out. The artifacts created by the recordings devices may be due to defective electrodes, line noise and high electrode impedance. On the other hand, physiological artifacts are represented, for example, by eye movements, cardiac activity and muscle activity [11].

For a better visualization, the signal has to pass through filtering and artifact removal. With the goal of noise elimination from the various artifacts, numerous approaches can be use. One of most used method is linear filtering which is capable of removing artifacts in certain signals where the overlapped frequency bands do not match with the range frequencies of the brain signals. In this case, usual is applied low-pass and high-pass filters [12]. Another technique example is spatial filtering

that resorts to a small number of new channels, that are a linear combination of the original ones, that filters the signal by reuniting information that is spread over the various EEG channels [12].

At this phase, the result is usually a low dimension vector suitable for translation into output commands with all the relevant information [2].

Classification

During this step, the resulting vector is passed to the feature translation algorithm for detection and classification of the discriminative features. This process will allow deciphering of the pacient's intentions into suitable commands for the output device [2][8].

Control interface

At last, the resulting ouput commands will operate the external device, providing functions such as letter selection, cursor control, robotic arm operation, or other [2][8].

2.1.2 BCI Control Signals

As described at the beggining of section 2.1, a BCI system monitors cerebral activity for the interpretation of intentions. For that purpose, the brain transmits control signals that after proper analysis and modulation will allow the required output [2]. Those computer interfaces are classified according with the origin of the recorded signal being divided into two categories: exogenous or endogenous. Exogenous BCI systems are related with neuronal activity caused by external stimuli, while endogenous systems are mainly influenced by brain rhythms and other potentials [13].

Exogenous BCI systems require minimal training since their control signals are easy to set-up. Such systems monitor SSVEPs (steady-state Visual Evoked Potencials) and P300 control signals that require only one EEG channel to be detected and possess a high bit rate of information. In regard to VEP signals, they represent brain signal modulations in the visual cortex, where SSVEPs occur in reaction to stimuli of a higher frequency and as result they are not as susceptible to lower frequency artifacts as eye blinking. On the other hand, P300 indicates positive peaks due to infrequent stimulus [2][13].

In contrast, endogenous BCI systems necessitate training where the subjects have to learn specific patterns that will after be translated by the computer system. Those type of systems are described as being conditioned by the users and specific mental tasks performances [2]. Thus, endogenous interfaces do not use any external stimuli what is particularly advantageous for patients without motor function [14]. The control signals monitored by those kind of BCIs are SCPs (Slow Cortical Potencials) that represent slow voltages shifts in the brain signals and sensorimotor rhythms that are related with motor imagery without any movement [2][13].

2.2 Neuroimaging Method - Electroencephalography (EEG)

The brain activity can be monitored by electrophysiological methods where the activity is generated by the exchange of information between neurons and electrochemical transmitters or by hemodynamic methods given that neural activity is controlled by alterations in cerebral blood flow and blood oxygenation that are detectable with fMRI (functional Magnetic Resonance Imaging) techniques [2][15].

In this section, electroencephalography, one of the methods for the measurement of the electrophysiological activity will be described in more detail.

2.2.1 EEG and Measurement System

Electroencephalography (EEG) is a non-invasive technique that measures the electric activity that occurs during synaptic excitations of the dendrites in the neurons with the use of electrodes placed on the scalp. The EEG signal is a result of the potential difference over time between signal or active electrode and reference electrode [2]. For this process, researchers felt the need to create a standard system for the positions of the electrodes, the 10-20 system.

The 10-20 international system is the recognised method used for uniform distribution of the EEG electrodes across the scalp, independent from the head size. The standard clinical setup uses only 19 electrodes (Fig. 2.2). Taking into account the anatomic structure of the brain, the standard setup does not allow recording of the signals from the mesial temporal structures. Thus, if the machine allows more recordings, it is recommended that an inferior temporal chain would be included in the 10-20 system performing a total of 25 electrodes (Fig. 2.3) [16].

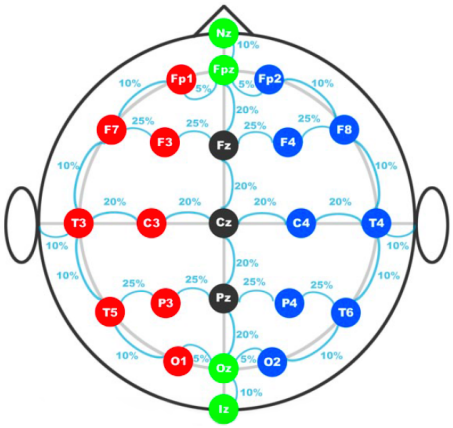

Figure 2.2: Standard 10-20 system with 19 electrodes [17].

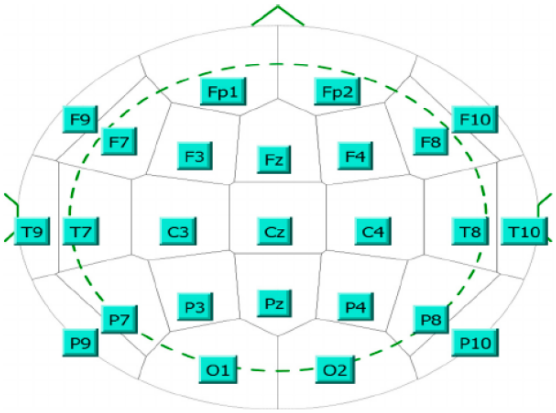

Figure 2.3: Recommended standard 10-20 system including the inferior temporal chain (T9/T10, F9/F10 and P9/P10) with 25 electrodes [16].

Due to an incomplete coverage of the scalp using the standard electrode configuration, it was also created a 10-10 system (Fig. 2.4) that allows a more complete recording of the patient brain activity. Despite the creation of this more complex method, the standard setup has the advantage of taking less time and being more efficient [16].

An electroencephalography system is composed by electrodes, amplifiers, A/D converter and a recording device. For a good acquisition of signal, this method often resorts to gel that will reduce the impedance for a better conduction between the skin and the electrodes which are usually made of silver chloride (AgCl). Some of the more recent portable EEG devices chose not to use gel and instead are composed by active "dry" electrodes. Those type of electrodes can be constituted with materials as titanium and stainless-steel. They may also have in their structure preamplification circuits or be incorporated with ultra-high input impedance in case of no active circuits (passive electrodes) [2].

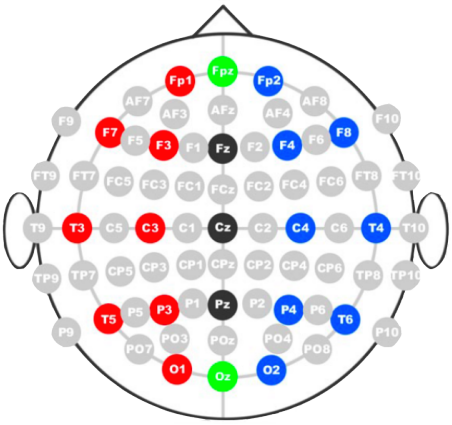

Figure 2.4: 10–10 Positioning System (modification of the 10-20 system) [17].

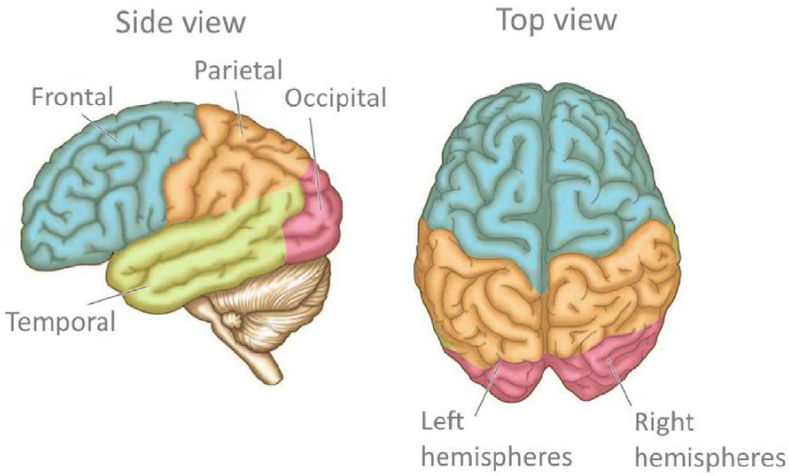

Figure 2.5: Locations of the different lobes - frontal, temporal, parietal and occipital [18].

2.2.2 Brain Anatomy

For a better understanding of the EEG signal and positioning of the electrodes across the scalp, it is important to study the different regions of the brain and their functions.

The human brain divides into four lobes: frontal, temporal, parietal and occipital lobes (Fig. 2.5).

Frontal Lobe

The frontal region is the largest of the brain, thus for a better analysis it is divided into different areas: dorsolateral, inferolateral, orbitofrontal and medial [19].

The dorsolateral frontal lobe is composed by the prefrontal cortex, the premotor

cortex and the primary motor cortex and its responsible for the motor tasks [19]. In respect to the inferolateral frontal region, the dominant hemisphere, usually the left side, is in charge of the expressive language [19]. Both orbitofrontal and medial frontal areas have as function the control of emotions, social interactions and personality [19].

This lobe is truly important in the field of concentration, orientation and judgement being involved in the process of difficult decisions and interactions [19].

Temporal Lobe

The temporal region includes the primary auditory cortex responsible for processing sound [19]. This area is also important in the retention of emotions, visual memory and language comprehension [19].

The medial area of the temporal lobe is composed by essential structures of the brain as the parahippocampal gyrus, uncus, hippocampus, tamporal horn and choroidal fissure [19].

Parietal Lobe

The parietal area of the brain is located between the occipital and frontal lobes and above the temporal lobe [20]. In this region is situated the primary somatosensory cortex [19].

This brain region is in charge of the primary analysis of somatic sensations as touch, position of the limbs and temperature [20]. This area is also responsible for the examination of space and specification of spatial target important in the motor taks [20]. Another functions of the parietal lobe is the generation of attention and the analysis of visual motion [20].

Occipital Lobe

The occipital lobe is the main area capable of processing the visual information and as a consequence, damages in this region can cause blindness and hallucinations [19].

This brain region is divided into three surfaces (medial, lateral, and basal) and three borders (superomedial, inferolateral, and inferomedial) [21].

2.2.3 Frequency Ranges

The EEG resulting signal can be filtered according to the different ranges of frequency: delta (δ), theta (θ), alpha (α), beta (β), and gamma (γ), respectively (Tab. 2.1).

Table 2.1: Frequency intervals of the different brain waves [22].

Brain Waves	Frequency Interval (Hz)
Delta, δ	0.1 - 4
Theta, θ	4 - 8
Alpha, α	8 - 13
Beta, β	13 - 30
Gamma, γ	30 - 70

Delta band (δ)

Delta waves are the lowest in the frequency band spectrum. They can be divided in two different groups. The lowest delta frequencies (<1 Hz) are related to cortical integration and regulation of the body while higher delta frequencies are a sign of cognitive processes as active memory [23]. They are more pronounced on the frontal region in adults and posteriorly in children [24].

Those waves have often maximal amplitude in the frontal regions and are usually only visualized in a deep sleep state in adults. If observed during an awake state, it's often a sign of neurological diseases [2].

A down side of delta waves is that, due to their low frequency, they are mistaken by artifacts signals [2].

Theta band (θ)

Theta waves are usually related to drowsiness, meditation [25], emotion, cognitive processes, memory and spatial processing [2]. In the theta domain, most of the observed frequencies are on the lower half of the interval, closer to 4 Hz, and are predominant on the temporal regions. The temporal theta represents verbal recall (left side) and spatial orientation (right side) [23].

In adults in a normal awake state, it is possible to observe a small amount of theta waves. However, in children or adults in a drowsy state, it can be observed a most

higher amount of theta frequencies. Likewise to the delta range, if a large set of theta waves are observed in awake adults, it is a sign of neurologic diseases [2].

Alpha band (α)

Alpha frequencies are related to visual processing and, sometimes, to memory brain functioning [2]. Recent studies show that alpha rhythms can occur in any part of the brain (as theta activity) but are mostly found in occipital (maximal) and frontal brain regions [2][23][25].

Over the time, another fact that was observed is that this band of frequency transmits also mental effort. When the eyes close and the body relaxes, the alpha amplitude increases and when the eyes open and there is mental effort they attenuate mainly in frontal areas [2].

Other important feature is that, in the same range as alpha frequencies, it can be found mu waves although they are connected with the motor cortex and, sometimes, are correlated with beta frequencies [2].

A consequence of aging is the slowing of alpha waves and combined with an increase of theta frequency, it can indicate cognitive decline and Parkinson's disease [23].

Beta band (β)

Beta waves are able to measure motor activity and are maximal on the frontal and central regions of the brain. When there is no motor activity they have a symmetrical distribution, whereas active movement results in the attenuation of the waves and change of the symmetrical distribution [2]. They are also related with cognitive processing and are stimulated into activity by gamma [23].

Due to the fact that beta brain waves are represented in a big frequency interval (13 - 30 Hz), usually for analysis the band is divided at least into two bands: low beta (13–21 Hz) and high beta (21–30 Hz) because of the differences in topographies and reactivity to tasks [26]. However, opinions may vary in relation to the amount of sub-bands and their limits frequency values [23].

Higher frequency beta waves are mostly found on the central region of the brain in the sensorimotor area (C3, Cz, C4) [27]. They are also known as rolandic beta frequencies and can possess a range of frequency of 14 to 30 Hz [27]. On the other hand, lower frequency beta waves are predominant on the frontal region of the brain (F3, Fz and F4 locations) and have a frequency maximum at around 19 Hz [27].

Those frequencies are more related with cognitive tasks and decision making [27].

Gamma band (γ)

This frequency range represents some motor functions, perceptions of visual and auditory stimuli and cortical processing related to cognitive functions [2]. Also, some studies reveal correlation between gamma and beta cortical oscillatory activity and force. Gamma waves are maximal during muscle contraction [2]. They are mostly found on the area of the somatosensory cortex [24].

Because of artifacts resulting from electromyography (EMG) or electrooculography (EOG), gamma frequencies are less used in EEG-based BCI systems [2].

The tab. 2.2) represents a summary of the characteristics from the differents brain waves.

Table 2.2: Summary of the brain waves features.

Brain Waves	Brain Regions	Features
Delta, δ	- Frontal (adults) - Posterior (children)	- Cortical integration - Regulation of the body - Cognitive processes
Theta, θ	- Temporal	- Drowsiness - Meditation - Emotion - Cognitive Processing - Memory - Spatial Processing
Alpha, α	- Occipital (maximal) - Frontal	- Visual Processing - Memory brain functioning
Beta, β	- Frontal - Central	- Motor Activity - Cognitive Processing - Decision Making
Gamma, γ	- Somatosensory Cortex	- Motor functions - Perceptions of visual and auditory stimuli - Cortical processing

3

State of the Art

In this chapter the work that has been done so far in the scope of drowsiness detection and the methods and equipment used for its research are described.

3.1 Research on Drowsiness Detection

Within the scope of drowsiness detection some research has been done mainly concerning the danger of falling asleep while driving. In begining stages, studies were done in the field of image processing, where images recorded by a video camera were analyzed according to the driver's face [28] or eyelids movement [29]. In 2002, an investigation was done using time series of interhemisphere and intrahemisphere [30]. The correlation between homologue electrodes, on the interhemisphere, allowed to observe a decrease with drowsiness [30]. On the intrahemisphere was possible to notice the transition from alertness to drowsiness and vice versa [30].

As the studies in the area developed, another strategy of decomposing the EEG into frequency sub-bands was explored. The changes of alpha and theta waves, during wakefulness, give information about the drowsy state of the subject. In an alert state, alpha power is usually low unless the subject is severely fatigued. On the drowsy state, alpha power is high. The transition from a condition of drowsiness to sleep represents a gradual alpha power reduction and a gradual increase of theta power [31]. Together with variations of the power of lower frequencies it was noted an increase of Shannon Entropy and K-L Entropy before driving that proved their sensitivity to sleepiness and importance on fatigue detection [3].

Bandwidth changes also showed to have an influence on the detection of awake and drowsy states as sporadic synchronization was dectected in the EEG signals while the subjects were trying to maintain wakefulness against sleepiness [32]. From the extration of some chaotic features, it was possible to conclude that the complexity of brain activity in alertness is higher than in drowsiness [33].

3.2 Data Acquisition

Over the years, EEG devices and techniques for data acquisition, within the scope of somnolence levels, have been developed according to the available technology needs and evolution of BCIs. Most of the papers about drowsiness detection use complex EEG systems with a large number of electrodes. Besides the normal EEG caps, some examples of EEG devices and sampling rates used in the past were the MEDELEC 1A97 EEG system with 16 channels and a sampling rate of 256 Hz per channel [30] and the Grass Model-78 Polysomnography[3] system with 25 channels avaiable and a sampling rate that can get to at most 1000 Hz [31].

With the advance of technology the need for different types of EEG devices emerged. Focus on portable wireless EEG systems increased in the last years like, for example, the B-Alert EEG System, with 10 to 24 channels, that was used in the field of drowsiness detection [34]. The developers of EEG portable devices are also working towards the goal of creating more affordable systems as is the case of the Emotiv system with 5 to 14 channels and the Muse headband with 4 channels[4].

Concerning the time acquisition matter, there is not a pre-established notion on which is the ideal recording duration for analysis. Within the scope of somnolence identification, different approaches were taken. For instance, a study using a neural network and wavelet coefficients resorted to the recording of seven hours episodes where EEG signals were taken every 20 minutes for each block and lately divided into five seconds epochs for examination [31]. Another paper resorting to instantaneous equivalent bandwidths for detection of drowsiness, acquired data from 30 minutes recordings in a shielded room and, subsequently, five minutes of raw EEG were selected from it for future evaluation [30]. A more recent research using the Muse headband sensing system recorded brain waves of each individual during one hour and proceeded to analyze 50 minutes from it [35].

3.3 Electrodes Position on the Scalp

For drowsiness detection the location of the electrodes, their impedance and the state of alertness are very important [31]. One of the problems in the scope of EEG research is the missing information about the methods for channel selection, lack of

[3] GRASS TECHNOLOGIES, https://www.erikg.com/grass.html, visited in 2019-04-02

[4] EEG Headset Prices – An Overview of 15+ EEG Devices, https://imotions.com/blog/eeg-headset-prices/, visited in 2019-04-02

justifications and different opinions [36].

A study for sleepiness recognition using the Emotiv EPOC headset containing 14 electrodes and two reference electrodes opted to chose six positions in the frontal lobe: AF3, AF4, F3, F4, FC6 and F8, and one in the parietal lobe: P8 for identification of alpha and beta pulses [25]. However, another paper selected the signal from the electrodes in the occipital regions O1 and O2, where it is highly correlated with the driver's alertness level [37]. Some authors decided also to use more electrodes for data acquisition as, for example, in cases of measuring the entropy of the brain where electrodes were positioned at 14 locations (F7, F8, T3, T4, T5, T6, F3, F4, C3, C4, P3, P4, O1, O2). This last article defended that during wakefulness, alpha and theta waves of interest for research on sleepiness [31]. Regarding the Muse system, the study found in the field of drowsiness detection used only the EEG recording from one of the frontal sensors for later examination [35].

3.4 Artifacts Removal

With the extration of the EEG data, an aspect that must be taken into account is the different artifacts of the recording. Besides roving eyes, artifacts may have other sources such as dangling legs, muscle tension, surrounding noise, teeth grinding, sweating, breathing, heart beat, or electrical line noise. All scalp locations are subject to contamination. The locations with more artifacts are, usually, the frontal (20–30 Hz range) and temporal (40–80 Hz range) at the Fp1, Fp2, F7, F8, T3 and T4 positions [23][38].

Methods for artifact removal are dependent on the type of data that was recorded and the goal. An important first step is to establish the frequency interval that we intend to study. An hypothesis for that is to use a band pass filter such as, for example, a butterworth filter [3] or a Chebyshev filter [33]. The next step is the removal of frequent biologial artifacts created as a result of blinking and movements, for instance. When EOG data is also available it is easy to remove visually movement artifacts [33]. Another strategy used was the independent component analysis (ICA) followed by a moving-average spectral analysis using a 250-point Hanning window with 125-point overlap [1]. To further minimize the artifacts effects, the resulting signal was filtered by median filter with a moving 2-s window [1]. For the artificial noise removal that results from the grounding of the EEG electrodes (50 Hz in Europe), it is usually used a notch filter [33].

One other technique used for artifact rejection was organizing the data by epochs according to the sum of square amplitudes and save the first, for example, 100 epochs with the lowest total amplitude for further analysis [39].

3.5 Methods for Data Analysis

After artifacts removal, different ways for the interpretation of the EEG signal for somnolence detection were already explored. Most studies resort to time series algorithms such as FFT, DWT and PSD for examination of the variation of amplitude over different frequencies. Besides those methods, nowadays, the interest in machine learning has been growing and some research using artificial neural networks has been done in the field of distinction between an alert and a drowsy state.

3.5.1 Time Series Algorithms and Feature Extraction

Since power spectral ranges are associated with fatigue and drowsiness, one viable way to separate the frequencies is to pass the filtered signal through a FFT [34] that will convert the signal to a frequency domain. Another method to separate the different frequency bands is to apply a DWT that allows the analysis with different resolutions by decomposing the signal by successive high-pass and low-pass filtering of the time domain signal. The studies that use the wavelet transform method defend that the Fourier transform is not ideal since it should only be applied to stationary signals, those do not change much over time [31]. However, althought the signal is continuous, from 0 Hz to half of the sampling frequency, the brain state of the person may originate some frequencies which are more dominant [4].

Regarding feature extration originated from time series algorithms, there is not an exact theory. In [31] was selected the range of frequency from 0.3 up to 70 Hz and after that examined the frequency interval from 1 to 30 Hz since it includes delta, theta, alpha and beta domains. However, [3] tested the frequencies from 0.5 Hz up to 45 Hz, also including a bit of the gamma spectrum. In [34], only the theta and alpha waves were investigated. From this, it is possible to conclude that studies, in the field of alert levels detection, opt to remove the beginning of the delta spectrum since it is more susceptible to artifacts [2]. Also, most papers choose not to select all of the gamma spectrum due to a higher probability of aliasing [40].

3.5.2 Feature Classification

After feature extraction, the next step is the process of classification by grouping them into different categories according to the similarities and differences between them [41].

Various techniques have been already proposed for drowsiness EEG signal classification. In [31] the approach of neural networks classification was taken, where the model that showed better accuracy results was the ANN configuration of 15-23-3, in which both layers had sigmoid transfer functions. The reason for using three outputs was for the representation of all scenatios: awake [0.9 0.1 0.1], drowsy [0.1 0.9 0.1] and sleep [0.1 0.1 0.9]. The targets of 0.1 and 0.9 were chosen, instead of 0 and 1, for preventing the outputs from being directly interpretable as probabilities. In that case, the total number of 294 samples was partitioned into: 198 samples for training, 44 for validation and 52 for testing.

In [35], methods for statistical classification in machine learning were implemented, SVM and LDA. The SVM technique is capable of constructing, in a multi-dimensional space, a hyperplane or a set of hyperplanes to obtain maximum separation between the classes. In respect to LDA approach, a pattern recognition is used for finding a linear combination of features which will separate classes of objects from each other.

Another paper, with the goal of somnolence detection, used fuzzy classification methods which are able to find the optimal structure and parameters automatically [1].

The tab. 3.1) represents a summary of the different techniques, described in this chapter, applied to the raw EEG signal for its processing and analysis.

Table 3.1: Summary of techniques used in EEG the signal analysis.

Artifacts Removal	Time Series Algorithms	Range of Frequencies (Hz)	Feature Classification
- By observation	- FFT	- 0.3 - 70	- Feed-Forward Neural Networks
- Bandpass filter	- DWT	- 1 - 30	- SVM
- Notch filter	- PSD	- 0.5 - 45	- LDA
- Moving average Hanning window with overlap			- Fuzzy Networks
- Median filter			
- Establishment of a threshold			
- ICA			

4

Experimental Setup

4.1 Wearable and Wireless EEG Devices - Muse headband

Recently the need for the creation of wearable and wireless EEG devices has increased for applications such as brain computer interfaces. Those EEG systems allow for the measurement of brain activity without the need of a hospital setup, making possible their application in day to day life [42]. Wireless equipments provide real-time recordings for immediate collection and interpretation of data important in cases such as drowsiness detection [5]. Those simpler devices use dry electrodes without the need for a conductive gel which is usually utilized for reducing the electrode impedance, allowing a better connection for brain waves detection [5]. However, dry electrodes are easier to place and if implemmented, for example, in a headband, simple to fixate.

The second version of the Muse headband was used with the purpose of recording brain activity. However, the third version of the Muse headband was launched into the market during the realization of this project. This last version of Muse available also provides information of the heart rate, breathing and body movements[5].

The Muse headband is capable of measuring, mainly, EEG signals by picking up variations on the electric field as they manifest as voltages on the surface of the scalp, with a dynamic range of [0; 1682,815]μV and a sampling rate of 256 Hz. This system has seven dry electrodes in which four of them read signals in the electrodes positions TP9, AF7, AF8 and TP10 (Fig. 4.1), according to the 10-20 modified system[6]. Regarding the composition of the electrodes, the frontal ones are coated with silver while the temporal pair is made with conductive silicone-rubber[7].

[5]Introducing Muse 2, https://choosemuse.com/muse-2/, visited in 2019-08-27

[6]Muse^{TM} headband, http://developer.choosemuse.com/tools/available-data, visited in 2018-10-07

[7]Myndlift clinical system, https://www.myndlift.com/myndlift-equipment, visited in 2019-07-05

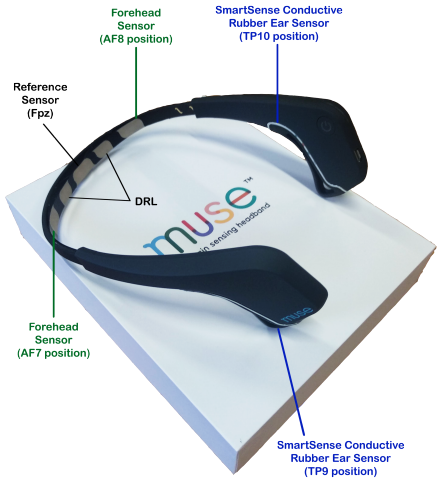

Figure 4.1: Muse headband, 2^{nd} version

This device has also 1 REF (reference electrode) and 2 DRLs (Driven Right Leg electrodes) in each side. The reference electrode provides a baseline measurement that is compared to every recording[8]. This electrode is placed on the Fpz position (center of the forehead), according to the 10-20 system[6]. As a supplement to the REF, the DRLs circuits, also known as ground electrodes, will supress the active noise by driving the reference through the skin and adjusting the ouput bases on noise feedback from the reference signal[6].

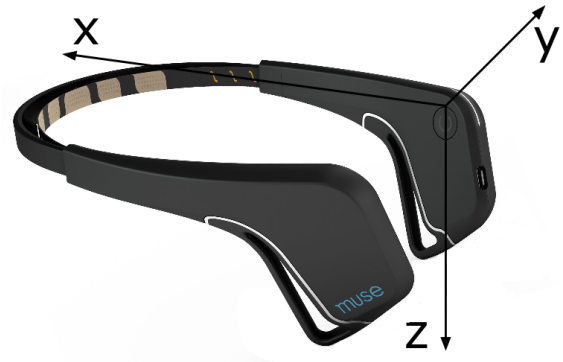

Figure 4.2: Accelerometer axes[10].

The Muse set has also an accelerometer and a gyroscope. On both of them, the directions X, Y and Z are oriented on a Right Hand Coordinate System where the X is pointing forward from the center of the head[7].The accelerometer measures 3 values (in milli-G's) that represent the acceleration in relation to the gravity in the

[8] Muse^{TM} headband, `http://www.forum.choosemuse.com`, visited in 2018-10-07

directions x, y and z, respectively (Fig. 4.2). Those values depend on the positions and movements of the head as, forward/back and up/down[6]. Thus, as the head leans down, aligning the X axis with the downward force of gravity, the X values increase[9]. However, if the head inclines upwards, the X values become negative. On the other hand, Y values increase if the head tilts to the right and decrease if the head bends to the left[9]. If the headband is on the level of the head, it will be in the direction of the ground aligned with the Z axis (X = 0, Y = 0, Z = 1)[9]. However, if the headband moves out from this orientation, the Z values will decrease[9]. In this case, if Z = -1 the headband is upside down.

As for the gyroscope data, it represents the rotation in degrees per second of the X, Y and Z directions (around 1000 degrees per second)[6]. The rotation around the X axis corresponds to movements of the head side to side [10]. Thus, when the head is tilting to the right, positive values increase. Motions up and down of the head represents rotation around the Y axis[10]. So, when the subject is looking up, Y positive values will increase. If the individual is looking to the left or right, there is rotation around the Z axis[10]. The Z positive values will increase if looking to the right.

This EEG portable device, in each session, starts with self-calibration protocols where instead of doing an average brain waves, it will calibrate to each subject. This procedure is really important for a better performance of the headband since the brain state is slightly different from session to session, there is a lot of different skull shapes and sizes and the brain morphology changes from human to human[8].

For a good performance of the Muse headband, it was important to clean the device. With use and time, electrodes could lose the ability of recording brain waves. This would happen due to the presence of dust or oil from the skin on the electrodes. Thus, it was important to use a cotton swab with rubbing alcohol to clean the sensors[11].

[9] LibMuse 6.0.3 - Accelerometer, https://web.archive.org/web/20181211073121/http://android.choosemuse.com/enumcom_1_1choosemuse_1_1libmuse_1_1_accelerometer.html, visited in 2019-08-28

[10] LibMuse 6.0.3 - Gyro, https://web.archive.org/web/20190515215757/http://android.choosemuse.com/enumcom_1_1choosemuse_1_1libmuse_1_1_gyro.html, visited in 2019-08-28

[11] How do I care for my Muse headband?, https://choosemuse.force.com/s/article/How-do-I-care-for-my-Muse-headband?language=en_US, visited in 2019-08-28

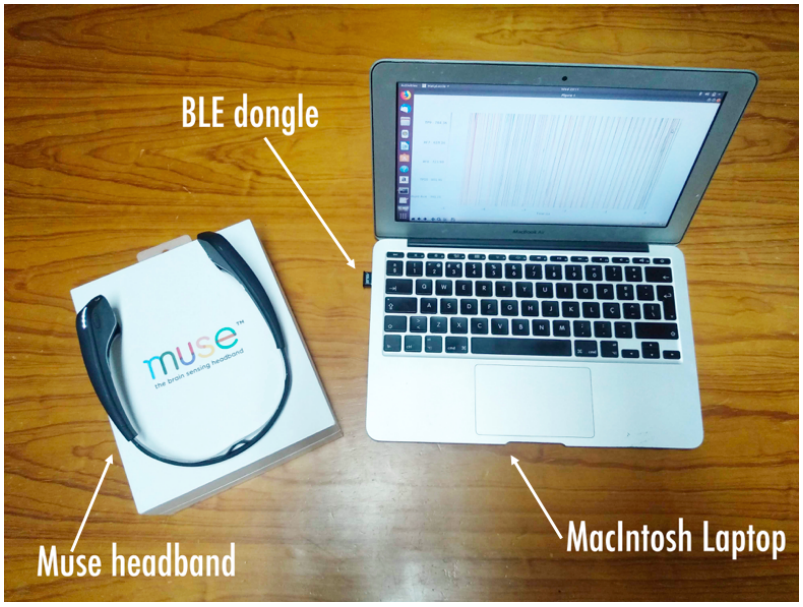

Figure 4.3: Material used for the EEG signal recording.

4.2 Connection Protocol

Muse is a portable system where the raw EEG signal is transmitted via Bluetooth Low-Energy (BLE) to a computer, in real-time. The computer used was a MacIntosh, with Mac OS X 10.10.5, equipped with a BLE dongle (Fig. 4.3) (Fig. 4.4). The MacIntosh computer was running Ubuntu 18.04.1 in a virtual machine so that the software could be developed in a Linux environment. Input data was parsed using Python 2.7.15, in the Linux virtual machine[12].

The BLE transmission corresponds to a low energy version of Bluetooth specified in the version 4.0. This version, with relatively short range, defends that sensors can communicate using a coin cell battery even up to two years [43]. This feature is promising in the field of wireless portable EEG devices since it allows the recording of the brain activity during bigger periods of time.

[12] Connection Protocol by Alexandre Barachant and Hubert Banville, `https://github.com/alexandrebarachant/muse-lsl`, visited in 2019-02-10

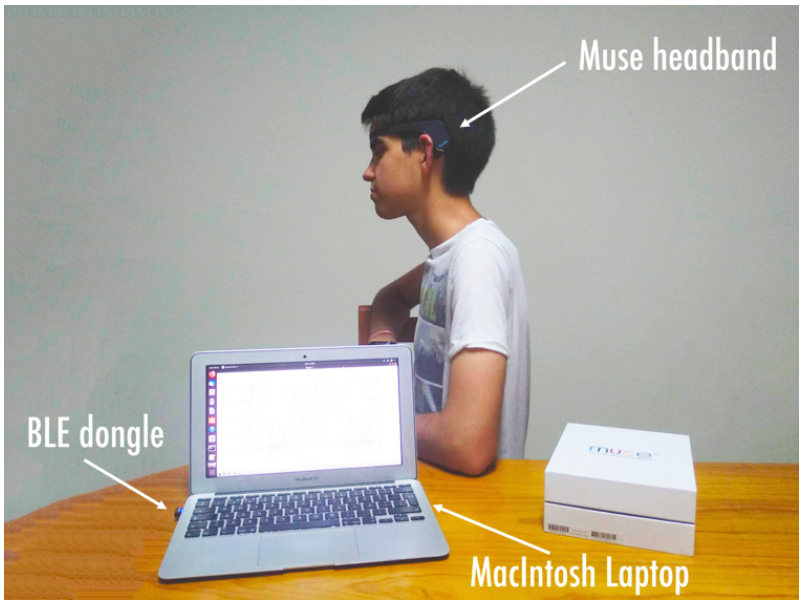

Figure 4.4: Experimental setup scenario for the recording of the EEG signal.

5

Methodology and Data Analysis

To achieve the proposed goals, a multi-step algorithm is necessary to obtain acceptable results. Thus, this chapter describes the steps of pre-processing of the EEG signal and features extraction for the databases contruction that will later be analyzed by a Neural Artificial Network model.

5.1 Pre-Processing of Data

For an improvement of the Neural Network outcome, the EEG signal was previously examined. The pre-processing of data allows minimization of the artifact influence. In this stage, it is also determined which interval of frequencies will be extracted to be fed to the ANN.

5.1.1 Data Acquisition and Time Synchronization

Firstly, the EEG signal, in both scenarios of alertness and drowsiness, was obtained from three subjects. For that, it was recorded eight minutes in each mind state. During the alert state recording the subject was alert and relaxed, whereas in the somnolence state recording, the subject was fatigued and relaxed.

After EEG signal acquisition with the Muse system, it was possible to notice that the timestamps were not constant. Those were created by the Interaxon API during processing of the bluetooth data and not by the hardware itself. Thus, during the EEG recording, bluetooth data stream was buffering and processing packets in chunks. That originated different time deltas between the obtained samples[13].

It was also observed that a lot of samples were missing. After some research it was possible to conclude that the reason for that still unknown and debatable. One

[13] Muse^{TM} headband, http://forum.choosemuse.com/t/syncing-time-between-muse-monitor-and-pc/1224, visited in 10-03-2019

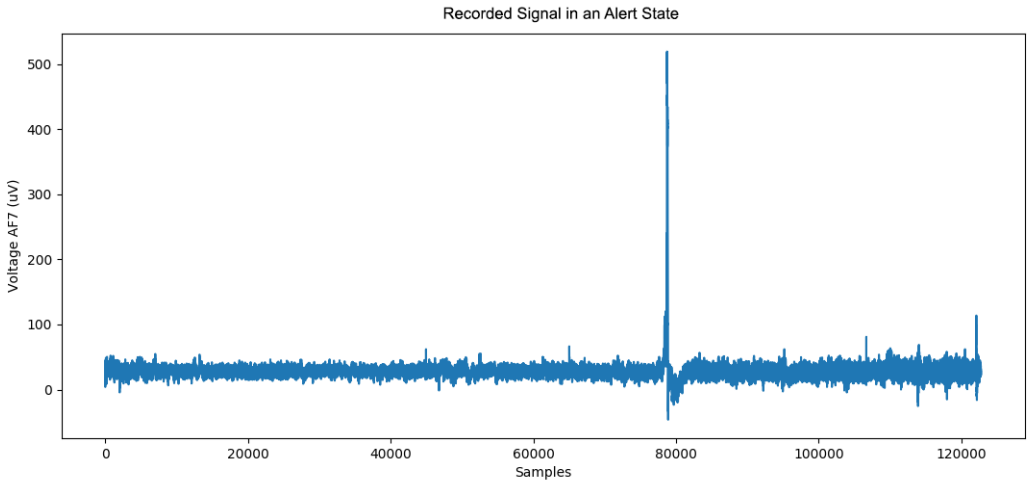

Figure 5.1: Recording of raw EEG, during eight minutes, captured by the sensor in the position AF7 in an alert state.

of the reasons could be that Muse recognize those samples as being eye blinks or similar artifacts [44].

To solve this problem and maintain a steady sampling rate of 256 Hz, it was calculated how many values were lost. With that it was possible the averaging of the deltas between timestamps keeping the 256 Hz sampling rate.

Fig. 5.1 represents an example of an eight minutes recording in an alert state. In this example, around 144 samples were lost (0,117% of the values).

5.1.2 Artifacts Rejection

A simple artifact removal was done. First, the more obvious artifacts, probably due to external noise and more harsh muscles movement, were removed by visual inspection (Fig. 5.2). This method of visual inspection was chosen since we are working with specific recordings to study the possibility of differentiate between two mental states. However, during a real-time situation, it could be applied a threshold. This feature can be used in the pre-whitening process of amplitude spectra [45]. It indicates which are the peaks limits (maximum and minimum) of the spectrum. Thus, the threshold will attenuate samples where the amplitude value is bigger than the established one. This way the most obvious artifacts wont be as pronounced.

After that, the five final minutes interval was selected for later analysis (Fig. 5.3).

Due to the fact that the brain state is constantly changing, the signal interpretation

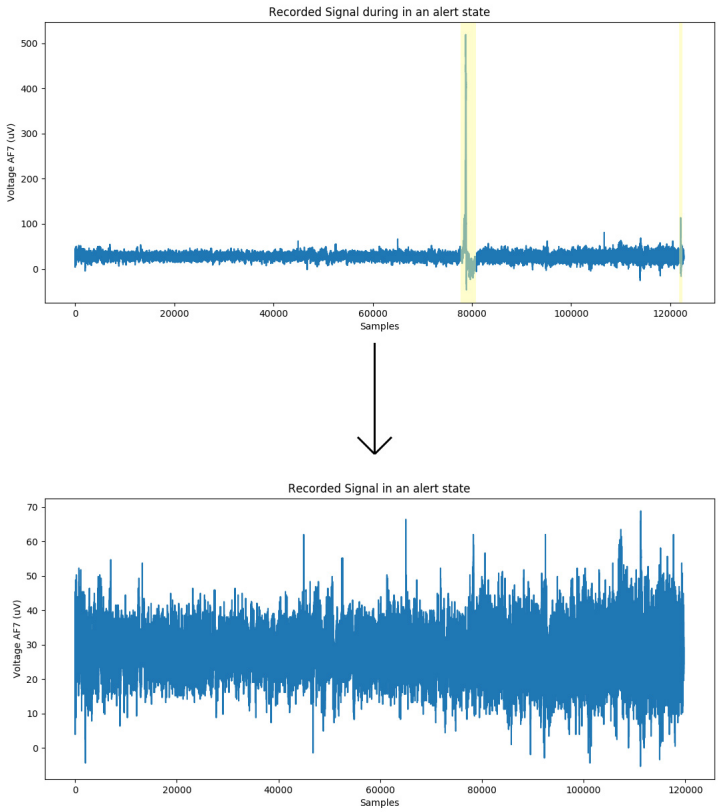

Figure 5.2: Removal of obvious artifacts in an EEG signal, captured by the sensor in the position AF7 in an alert state, by visual inspection.

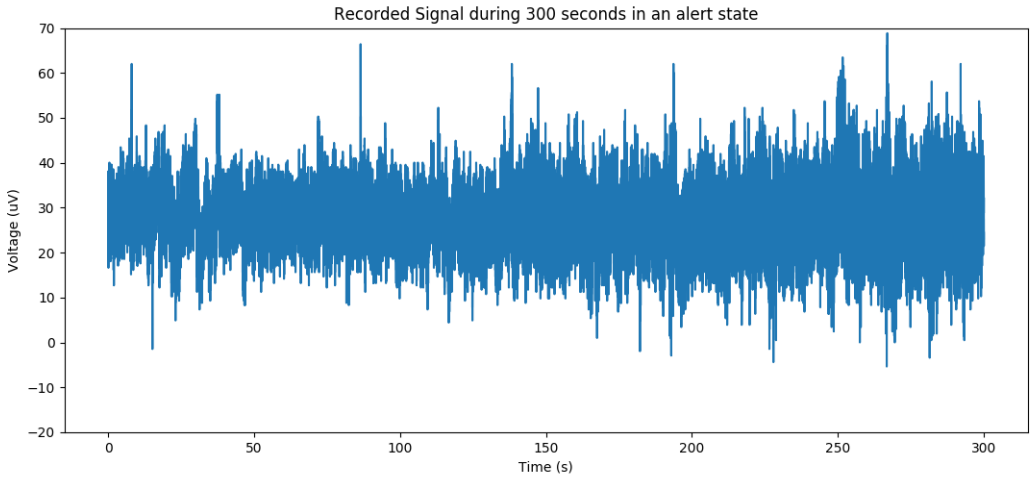

Figure 5.3: Selected five minutes signal for further analysis of EEG captured by the sensor in the position AF7 in an alert state.

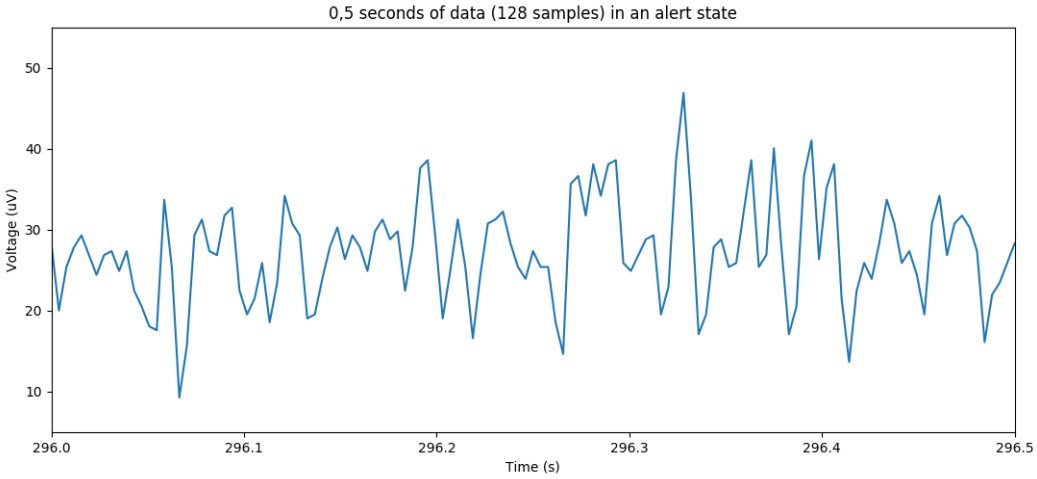

Figure 5.4: EEG during half a second in an alert state measured by sensor in the position AF7.

Table 5.1: Different frequency intervals tested.

Frequency Range (Hz)	Frequency Waves
1 - 21	δ, θ, α, low - β
1 - 30	δ, θ, α, β
4 - 13	θ, α
4 - 30	θ, α, β

was done taking into consideration changes with half a second interval (Fig. 5.4). Thus, each interval is composed with 128 samples ($256/2 = 128$). To further minimize the artifact influence in the recording, it was implemented a median filter to each half a second interval (Fig. 5.5).

Then, an order 6 bandpass filter (Fig. 5.6), which selects a specific frequency range to pass a signal unattenuated [46], was applied to each interval. Different frequency intervals were tested based on the influence of the different bands (Tab. 5.1).

A notch filter was also implemented. This method has the particularity of removing only a frequency passing the components below and above it [47]. Since the study of drowsiness detection has in focus the lower side of the frequency spectro, frequencies above 40 Hz were not analysed. With that said, there was no need to use the notch filter for the removal of the mains frequency oscillations of alternating current that, in Europe, is 50 Hz. But, this filter was applied to remove a 22 Hz frequency caused also by the power line frequency influence.

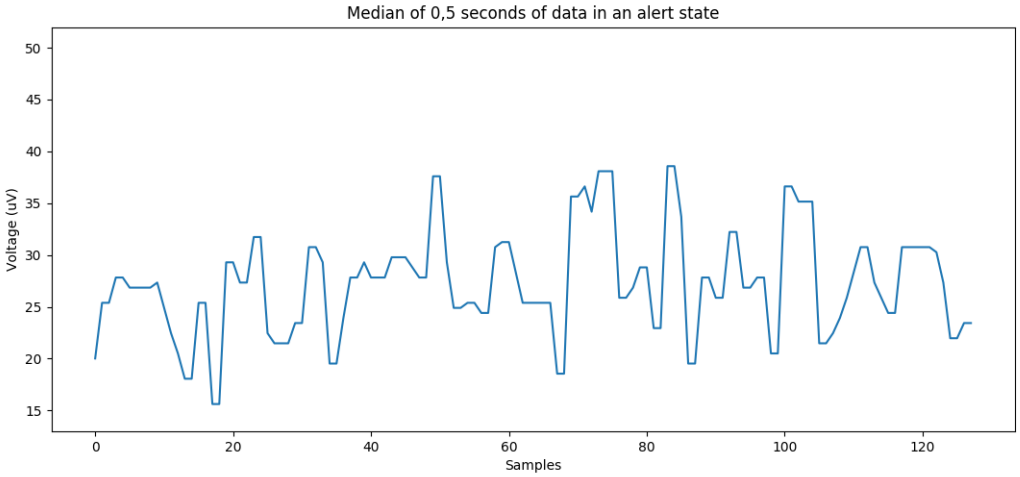

Figure 5.5: Median of EEG during half a second in an alert state measured by sensor in the position AF7.

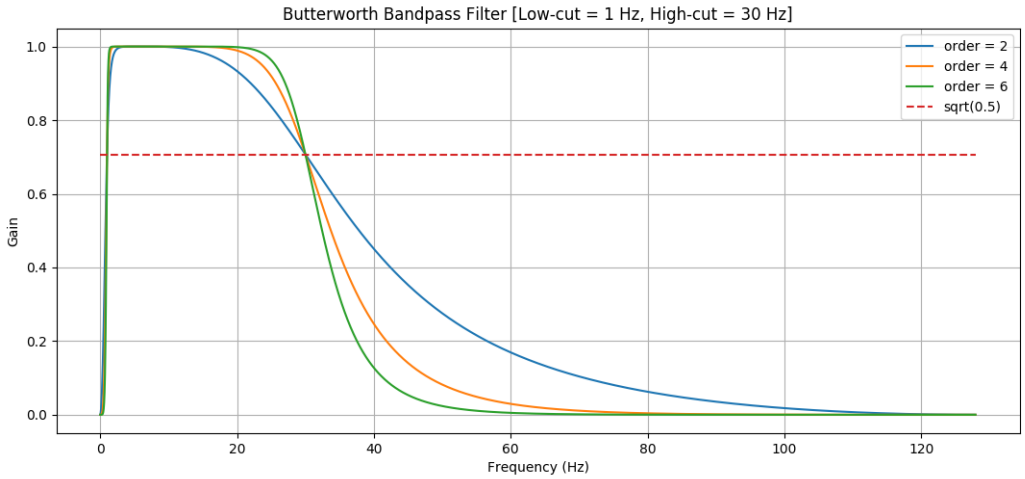

Figure 5.6: Representation of different frequency responses orders with Butterworth bandpass filter application for [1, 30] Hz.

5.1.3 Analysis with Time Series Algorithms

For the examination of the EEG signal, it is important to convert its original time domain to a frequency domain. The Fast Fourier Transform (FFT) performs a highly efficient computation of the Discrete Fourier Transform (DFT) of data samples series and from there it allows the power spectrum analysis [48]. The DFT maps a signal represented as a time series $x(n)$ into the frequency domain where its samples are equally spaced (Nyquist samples) [49].

The N-point DFT of a series is:

$$X(f_k) = \sum_{n=0}^{N-1} x[n] e^{-j2\pi f_k n} \tag{5.1}$$

for $f_k = k/N, k = 0, 1, ..., N-1$; N: number of samples

For real series, the real part of (Eq. 5.1) is symmetric at the folding frequency ($f_f = f_s/2$) while the imaginary part is antisymmetric. Those features represent the fact that the Fourier coeficients between $N/2$ and $N-1$ can be viewed as the negative frequency harmonics between $-N/2$ and $N-1$. Thus, the FFT negative part of the spectrum can be ignored [50].

$$|X(f_k)| = |X(\frac{k}{N})| = |X(k)| = |\sum_{n=0}^{N-1} x[n] e^{-j2\pi f_k n/N}| \tag{5.2}$$

for $f_k = k/N, k = 0, 1, ..., N-1$; N: number of samples

The DFT magnitude at bin k is correspondent to the FFT magnitude at bin k (Eq. 5.2).

As said in Chapter 4, the Muse headband frequency rate is 256 Hz. Since the signal has been analysed in half a second intervals, each FFT is composed by 128 samples and given that the spectrum is symetric, 65 samples are represented in the frequency domain, this is $N = 128/2 + 1$ (origin point) (Fig. 5.7). Since frequencies above the folding frequency (65 Hz) were not being considered in the study, this downsampling process did not affect the signal information given that, according to the Nyquist sampling theorem, aliasing can occur in the downsampled signal in frequecies higher than the folding frequency [40].

The Power Spectral Density was also determined to study how the power of the

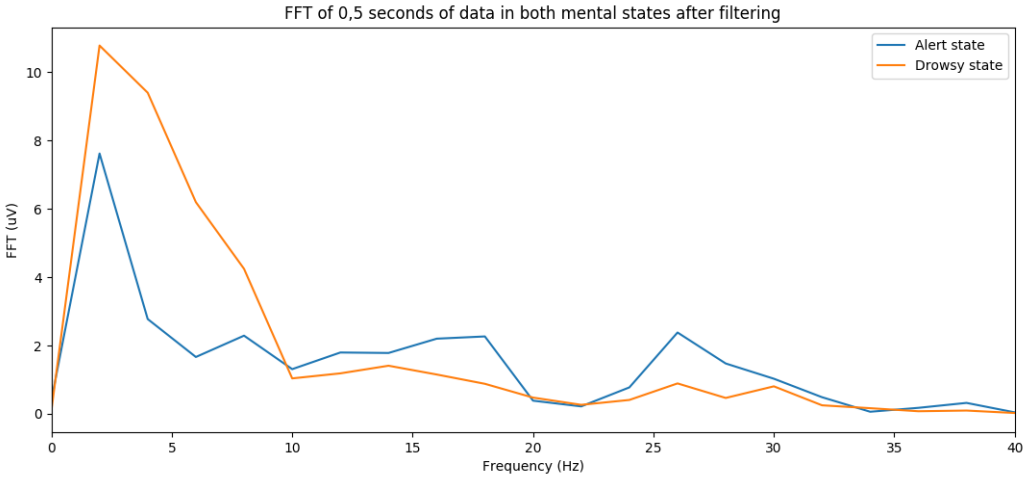

Figure 5.7: Filtered Fast Fourier Transform with bandpass filter from 1 Hz up to 30 Hz (interval of frequencies [0, 40] Hz), of half a second interval, in both alert and drowsy states, measured by the electrode in the position AF7.

EEG signal is distributed over the frequency (Fig. 5.8). The PSD was obtained by the square of the FFT amplitude (Eq. 5.3) where the obtained plot of each half a second is known as periodogram [51].

$$|P(f_k)| = |X(f_k|^2 \tag{5.3}$$

For a more in dept study of the disparities between the power spectral densities and the presence of the various brain waves of both vigilant and somnolent conditions, Welch's method was implemented. This procedure estimates the PSD by splitting the data into overlapping segments by computing a modified periodogram for each segment and performing the average of the overall periodograms[14]. This technique was applied with a sampling frequency of 256 Hz (one second) and an overlap of 50% (128 points).

Over the obtained PSDs overlapped spectra, a hanning window was also used (Fig. 5.9). The hann function (Eq. 5.4) has the purpose of smoothing discontinuities at the start and end of the sampled signal[15]. This windowing technique was used for atenuation of, mainly, the delta waves amplitudes (beginning of the spectrum) that are more susceptible to artifacts, as described in Chapter 2, and also to smooth

[14] Welch's Method Python, `https://docs.scipy.org/doc/scipy-0.14.0/reference/generated/scipy.signal.welch.html`, visited in 2019-07-15

[15] Hanning Window Python, `https://docs.scipy.org/doc/numpy/reference/generated/numpy.hanning.html`, visited in 2019-07-15

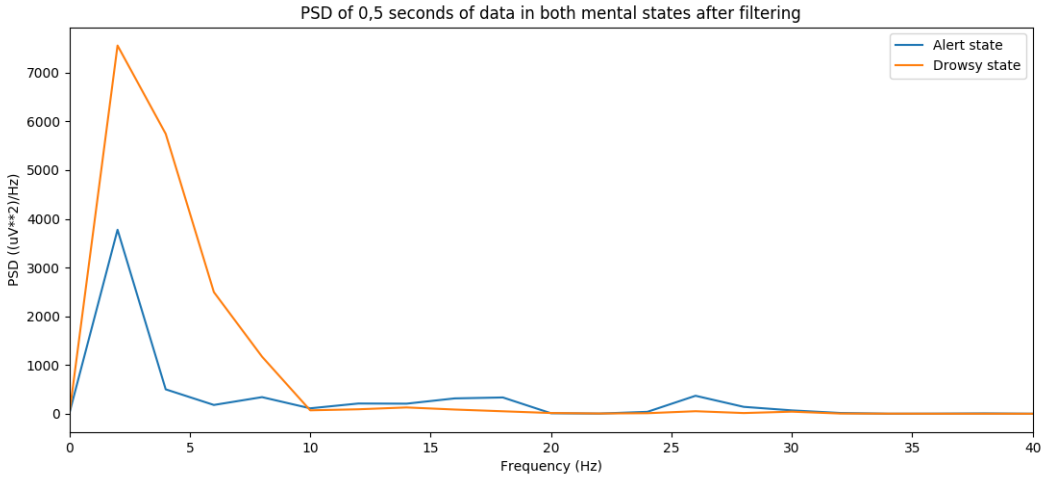

Figure 5.8: Filtered Power Spectral Density with bandpass filter from 1 Hz up to 30 Hz (interval of frequencies [0, 40] Hz), of half a second interval, in both alert and drowsy states, measured by the electrode in the position AF7.

gama frequencies not as important to this study.

$$w(n) = 0.5 - 0.5cos(\frac{2\pi n}{M-1}) \tag{5.4}$$

for $0 \leq n \leq M-1$; M = Number of samples

After averaging both PSDs in an alert and drowsy states during five minutes, the absolute and relative power of the various brain waves were obtained. For that purpose, the limits of the different frequency ranges were established. After, the Simpson's rule (Eq. 5.5[16]) was applied. This method uses a quadratic polynomial on each interval (1 Hz) to approximate the function and compute the integral[16].

$$S_N(f) = \frac{\Delta x}{3}\sum_{i=1}^{N/2}(f(x_{2i-2}) + 4f(x_{2i-1}) + f(x_{2i})) \tag{5.5}$$

for $[a,b], \Delta x = (b-a)/N, x_i = a + i\Delta x$; N = Number of intervals

The Simpson's rule is able to decompose the area under the line of the power plot into numerous parabolas and then sum it all[17]. However, this approach requires an even number of intervals. Thus, when the number of intervals were odd, the first $N-2$ intervals were obtained with the Simpson's rule and the last interval with

[16] Simpson's Rule, https://www.math.ubc.ca/~pwalls/math-python/integration/simpsons-rule/, visited in 2019-09-05

[17] Compute the average bandpower of an EEG signal, https://raphaelvallat.com/bandpower.html, visited in 2019-05-20

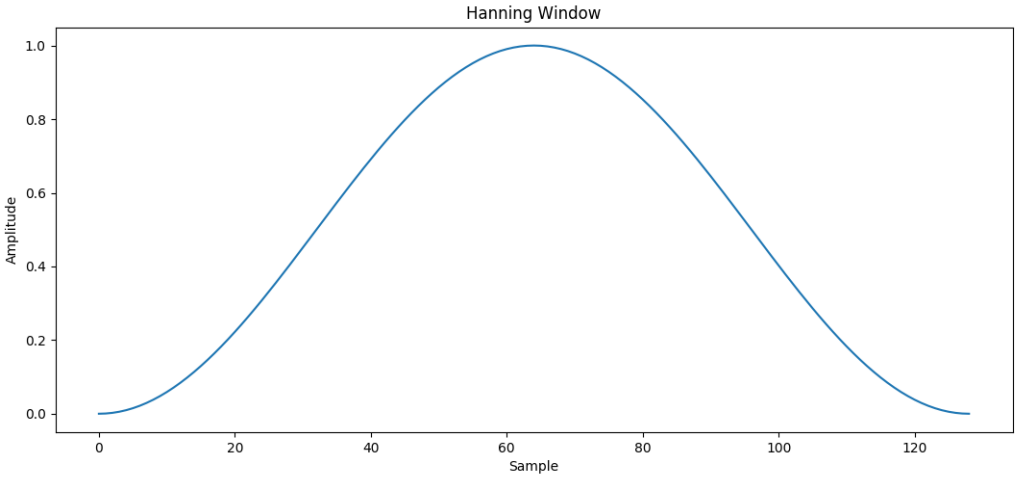

Figure 5.9: Hanning Window with 129 points applied to the resulting Power Spectral Density of EEG signal.

the trapezoidal rule[18]. The trapezoid rule (Eq. 5.6[19]) gives an approximation of an integral by summing the areas of the trapezoids[19].

$$T_N(f) = \frac{\Delta x}{2} \sum_{i=1}^{N} (f(x_i) + f(x_{i-1})) \tag{5.6}$$

for $[a, b], \Delta x = (b - a)/N, x_i = a + i\Delta x$; N = Number of intervals

Thus, the absolute power is the direct result from the area of the plot in the respective frequency interval while the relative power is acquired with the division of the corresponding brain waves absolute power by the total absolute power from all the brain frequencies.

With the values from the absolute powers of each brain waves were calculated the ratios between the theta and alpha frequencies (Eq. 5.7).

$$\theta, \alpha\, ratio = \frac{\theta\, absolute\, power}{\alpha\, absolute\, power} \tag{5.7}$$

[18] SciPy.org - scipy.integrate.simps, https://docs.scipy.org/doc/scipy/reference/generated/scipy.integrate.simps.html, visited in 2019-09-05

[19] Trapezoid Rule, https://www.math.ubc.ca/~pwalls/math-python/integration/trapezoid-rule/, visited in 2019-09-05

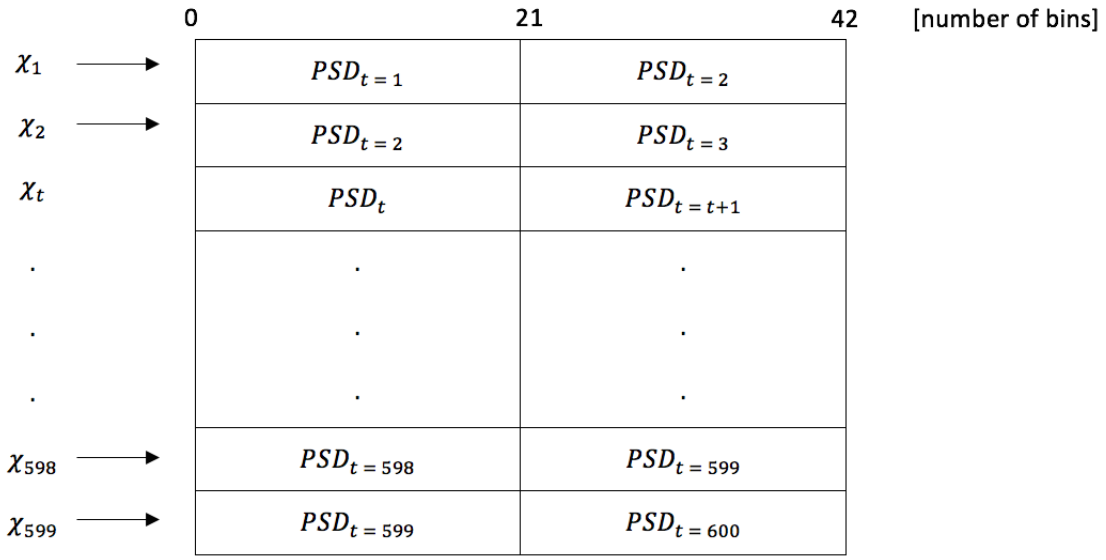

Figure 5.10: Exemplification of dataset construction of one mind state. Each section (ex. $PSD_{t=1}$) corresponds to the PSD spectrum [0, 40] Hz of a half a second interval and is composed by 21 bins.

5.2 Dataset Construction and Network Parameters

The filtered PSD data was later used for creating a dataset. Each dataset feature vector, that would further be used as the ANN input, was composed with 42 bins. This vector was composed with a total of one second of PSD filtered data. Thus, the first half of the vector (21 bins) was constituted with the PSD spectrum obtained from a half a second interval whereas the second half corresponded to the posterior interval. As said in the previous section, each PSD spectrum comprised frequencies from 0 up to 40 Hz. Thus, each bin has the information of 2 Hz. This resolution has to do with the fact that each interval corresponds to half a second. So, as the number of samples decreases to half so as the number of bins ($40/2 + 1 = 21$).

A 50% overlap was applied. Hence, the first half of each input vector was set up with the same data from the last half of the previous input vector. In summary, from each five minutes EEG recording (300 seconds) resulted a 1198×42 dataset where 599 features vectors represented the alert condition and the other 599 vectors the drowsy state. A last column was added for the outputs in which, the alert state was represented by 1 and the drowsy state by 0.

The diagram represented in Fig. 5.10 aimes to clarify the dataset construction of the data from one mind state.

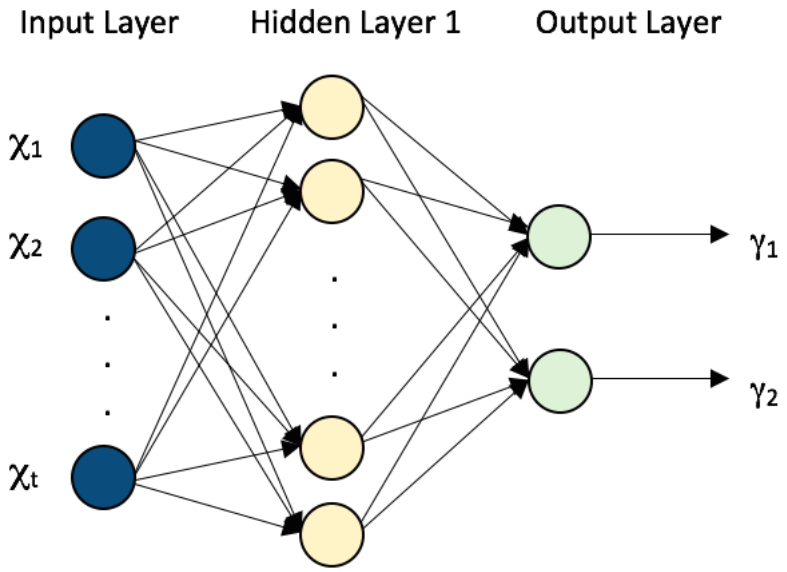

Figure 5.11: Neural Artificial Network model used.

Table 5.2: Different structures tested for the neural network.

Neural Network structures (Input layer - Hidden layer - Output layer)
42 - 5 - 2
42 - 10 - 2
42 - 20 - 2
42 - 42 - 2

The constructed dataset was then fed to an artificial neural network. The data was divided 80% for the training set and 20% for the test set. 20% of training data was separated for validation. The training set was constitued by 766 samples, the testing set by 240 samples and the validation set by 192 samples.

Regarding the structure of the network, it was composed by an input layer, one hidden layer and an output layer (Fig. 5.11). The number of inputs in the first layer was fixed to 42 and the output layer was constitued by two outputs. The reason why it was chosen two outputs was for better observe the precision of the neural network. For the hidden layer, different tests were performed to observe how many neurons would deliver the best result (Tab. 5.2). The input layer used a linear activation function and the hidden layer used a sigmoid activation function.

Fig. 5.12 represents a summary of all the methods applied for data analysis.

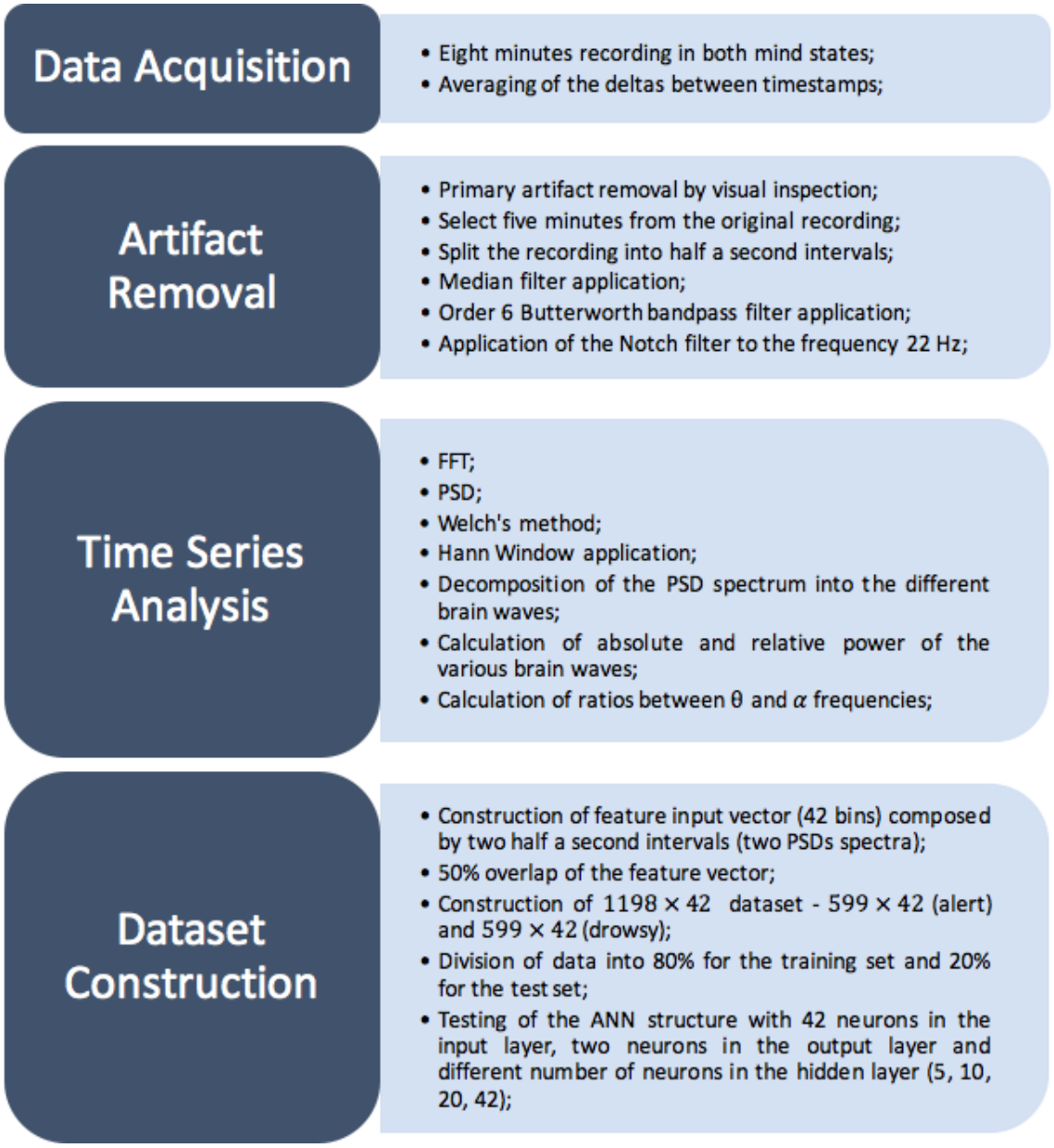

Figure 5.12: Methods summary.

6

Results

In this chapter the results from the EEG signal recordings and the application of the methods referred in Chapter 5 are described and interpreted. The viability of the artificial neural network model is tested according to the accuracy obtained.

6.1 Examination of Power Spectral Densities

First, analysis of the obtained power spectral densities was done. From the visualization of the averaged PSDs plot originated with the Welch's method application (Fig. 6.1), it is possible to notice that in the lower range of frequencies (delta, theta and beta), both states present similiar values. However, a slight dominance of the drowsy state is observed. Concerning the higher frequencies (beta and gamma) the alert state presents higher values.

The Welch's method is based on the average of absolute power densities, direclty proportional with the captured EEG signal. Thus, the absolute power values are highly dependent on the signal quality. The EEG recording is affected by the headband maintenance, electrodes position and contact with skin, different types of skulls, surrounding noise, skin properties and others. Therefore, different recordings can present high dispersions. In Fig. 6.2 is possible to notice that the drowsiness detection using the direct absolute power values is not trustworthy. With the observation of the subject 2 plot, it is noticeable a slight predominance of the drowsy state. However, the subject 3 plot presents a strong predominance of the alert state. Both of this situations represent a case of different quality of signals.

The Tab. 6.1 confirms the unreliable conclusions with the use of the direct absolute power values. As said before, in subject 1, the absolute powers of both mental states are around the same range of values due to the fact that the position and condition of the headband was really similiar. It is possible to observe in this subject that lower frequencies (delta, theta and alpha) are predominant on the drowsy state.

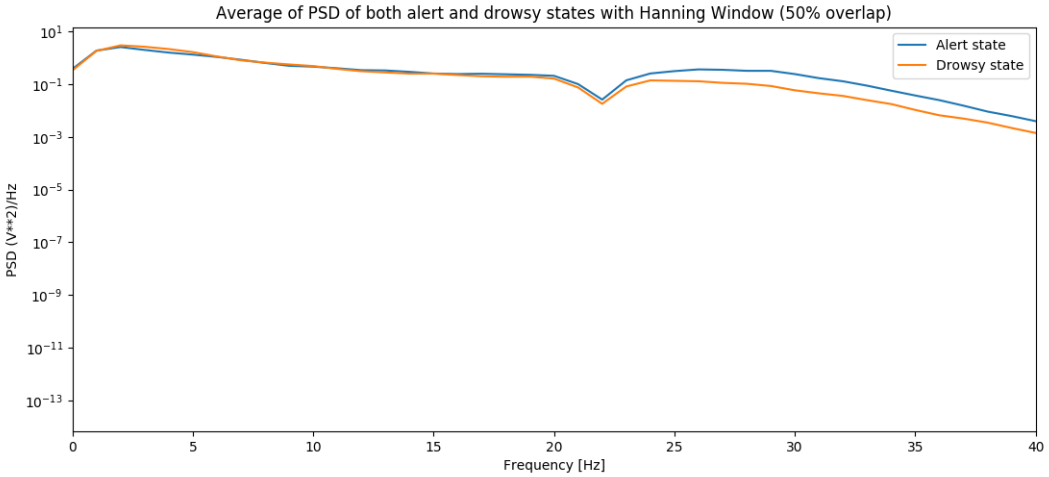

Figure 6.1: Resulting averaged PSD in both alert and drowsy from the application of the Welch's method with an overlap of 50% (Subject 1).

Table 6.1: Absolute powers of the various brain waves in both alert and drowsy states (values represented in (μ^2)).

	Subject 1		Subject 2		Subject 3	
Brain Waves	Alert	Drowsy	Alert	Drowsy	Alert	Drowsy
δ	6.396	7.706	63.797	621.071	196.682	5.063
θ	4.287	4.879	110.768	316.593	128.827	4.042
α	2.138	2.163	578.770	652.420	539.435	6.202
β	4.126	2.484	736.422	810.823	687.174	9.785
γ	0.641	0.177	308.414	307.595	280.514	3.620

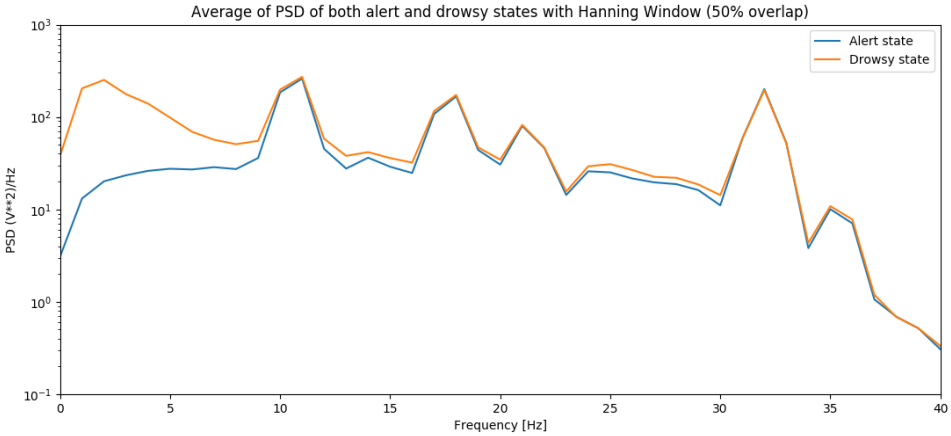

(a) Subject 2

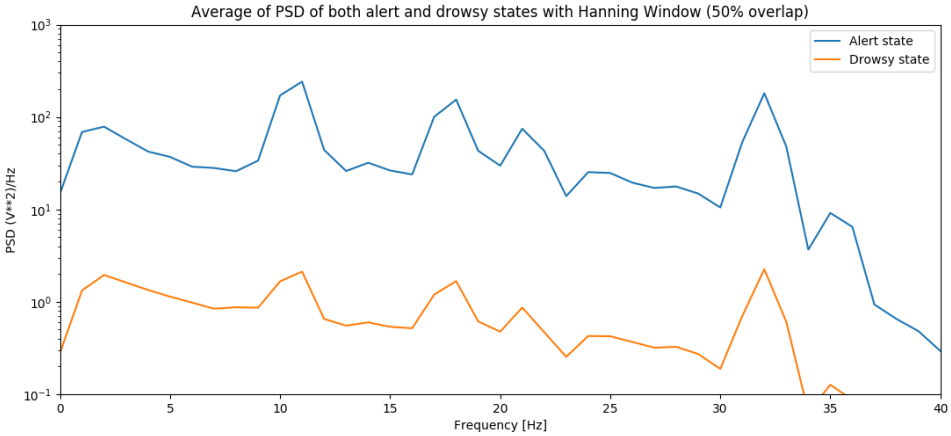

(b) Subject 3

Figure 6.2: Resulting averaged PSD in both alert and drowsy from the application of the Welch's method with an overlap of 50% (Subject 2 and 3).

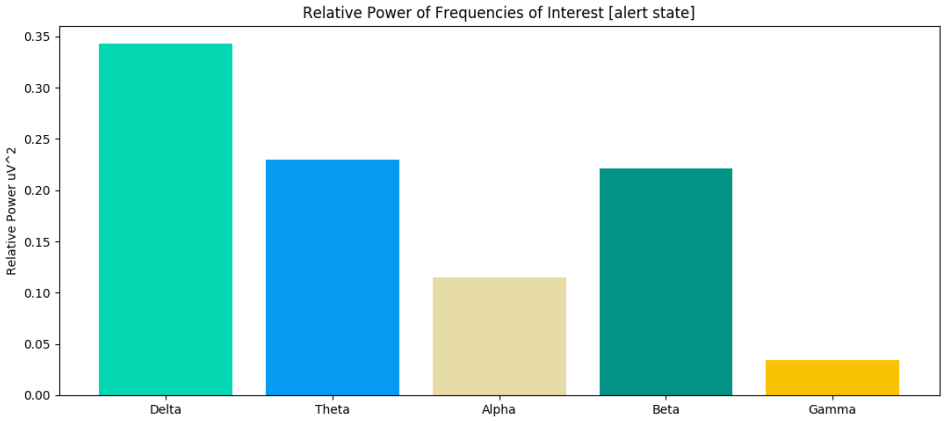

(a) Alert state

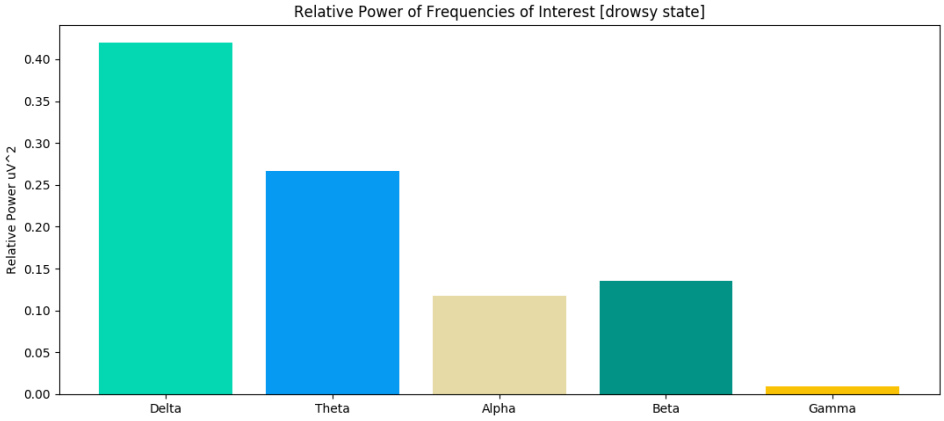

(b) Drowsy state

Figure 6.3: Relative power of the brain waves over five minutes of both mental states (Subject 1).

On the other hand, the higher frequencies (beta and gamma) are more present on the alert state. However, in subject 2 and 3, the discrepancies between the values of each state are truly noticeable, mainly in subject 3, due to different conditions during the EEG signal recording.

Nevertheless, the Welch's method and absolute powers allows for the achievement of the relative power values. The relative power represent the relation between the brain waves predominance and the total power of the spectrum. This feature represents a more reliable way to visualize the different frequency waves presence. Both bar plots represented in Fig. 6.3 are related to the subject 1. Lower frequency waves (delta, theta and alpha) are, as expected, more predominant on the drowsy state. Regarding the higher frequencies, they are more presentont the alert state.

Table 6.2: Relative powers of the various brain rhythms in both alert and drowsy states.

	Subject 1		Subject 2		Subject 3	
Brain Waves	Alert	Drowsy	Alert	Drowsy	Alert	Drowsy
δ	0.343	0.420	0.036	0.221	0.106	0.171
θ	0.230	0.266	0.062	0.113	0.069	0.136
α	0.115	0.118	0.323	0.232	0.290	0.210
β	0.222	0.135	0.411	0.286	0.369	0.331
γ	0.034	0.010	0.172	0.110	0.151	0.122

Table 6.3: Ratios obtained from the absolute powers between theta and alpha brain waves.

	Subject 1		Subject 2		Subject 3	
Ratios	Alert	Drowsy	Alert	Drowsy	Alert	Drowsy
$\frac{\theta}{\alpha}$	2.005	2.255	0.191	0.485	0.239	0.650

The Tab. 6.2 represents the obtained relative powers for all subjects. Concerning the subjects 2 and 3, the lower frequencies δ and θ are more predominant on the drowsy state and the higher frequency brain waves β and γ are more present on the alert state. However, contrary to the subject 1, alpha frequencies are superior on the alert state. As described in Chapter 2, α waves are highly related with the relaxation of the subject. Thus, in both tested mind states (alertness and drowsiness) the subjects were relaxed what can result in ambiguous results. Hence, it is possible to notice a higher correlance and better identification of drowsiness with delta and theta frequency waves. Regarding the subject 1 and the predominance of alpha frequencies on the drowsy state, it is mentioned in the BCI and Brain Waves chapter that, a consequence of aging is the slowing of alpha waves. Thereby, this subject was the older one with 49 years old in comparison with the other two subjects with 23 years old.

With examination of the Tab. 6.2, it is also possible to notice that the sum of the relative powers of the brain waves in each mind state is different than 1 as it would be expected. As explained on the chapter 5, this has to do with the fact that the Simpson's rule delievers an **approximation** of the area under the line of the power plot. Thus, since the area is an approximation so it will be the absolute and relative power values.

As described on chapter 3, delta waves are more susceptible to artifacts thus, it's

conclusions may not be as reliable. Therefore, between the other brain frequencies, the ones who showed, so far, correct and more pronounced drowsiness detection was the theta waves. Hence, the ratios between the theta and alpha waves were calculated for each subject. With Tab. 6.3 examination is possible to observe a higher theta to alpha ratio on the drowsy state, as it would be expected.

6.2 ANN Performance and Selection of the Best Model

As a complement to the absolute and relative powers and ratios analysis, different models of artificial neural networks were tested. In scenarios where there are numerous datasets this method is more advisable. This technique was explored on this project to study the reliability for drowsiness detection. If proven accurate, ANNs can be better explored in the future with a higher quantity of datasets.

First, as described on chapter 5, different frequency bands were tested at the step of bandpass filtering. With the PSDs obtained from the readings of the electrode AF7 from subject 1 and an artificial neural network structure $42 - 10 - 2$, it was possible to observe that the best accuracy was deliever by the frequency range from 1 Hz up to 30 Hz (Tab. 6.4). The obtained test accuracy was of 73,8%. This frequency interval includes δ, θ, α and β frequencies. Intervals including the gamma frequencies were not tested because they are not really significant for the drowsiness detection goal.

Table 6.4: Testing of different frequency ranges from the subject 1 EEG signal captured from the AF7 electrode. The ANN structure used was $42 - 10 - 2$.

Frequency Range (Hz)	Test Accuracy (%)	Train Accuracy (%)
1 - 21	54,2	72,3
1 - 30	73,8	81,3
4 - 13	53,1	68,6
4 - 30	71,7	80,5

Afterwards, various ANN structures were tested with the obtained PSDs from the subject 1 EEG signal captured by the AF7 electrode. With Tab. 6.5 examination, it is possible to notice that the ANN structure with better accuracy was $42 - 5 - 2$ with 74,2%.

Regarding the position of the electrodes, it was study which one delievered the best accuracy results. For that, PSDs originated from the recordings of the subject 2 were

Table 6.5: Testing of different ANN structures using the resulting PSD spectra with bandpass filtering of frequencies [1, 30] Hz. Data from the subject 1 EEG signal captured from the AF7 electrode.

ANN Structure	Test Accuracy (%)	Train Accuracy (%)
42 - 5 - 2	74,2	75,7
42 - 10 - 2	73,3	77,5
42 - 20 - 2	71,2	80,1
42 - 42 - 2	68,8	82,8

Table 6.6: Testing of different PSD spectra with bandpass filtering of frequencies [1, 30] Hz resulting from various electrode positions. The ANN structure used was $42 - 5 - 2$ with data from the subject 2 EEG signal.

Electrode Position	Test Accuracy (%)	Train Accuracy (%)
AF7	75,8	81,5
AF8	55,4	65,6
FRONTAL	69,2	72,4
TP9	76,7	77,8
TP10	78,8	83,1
TEMPORAL	76,2	79,3
ALL	57,1	70,9

used. The various electrode positions, AF7, AF8, FRONTAL $((AF7 + AF8)/2)$, TP9, TP10, TEMPORAL $((TP9 + TP10)/2)$ and ALL $((AF7 + AF8 + TP9 + TP10)/4)$, were tested (Tab. 6.6). Despite the fact that the temporal sensors presented high accuracy, it was selected the left frontal measure point, AF7, for further analysis. This decision was due to the reason that both temporal electrodes showed a big quantity of artifacts resulting in a high percentage of false positives. One of the causes for the high presence of artifacts in the back electrodes is the fact that their material is different from the frontal ones since they are made with silicone-rubber. This conductive material is used because of its streching capacity. However, this feature may lead to a loose electrode and as consequence poor contact with the skin [52]. Another reason was the location of the sensores in the head where there was the possibility of presence of hair that would also contribute to the loss of contact with the skin.

Lastly, the classification of all subjects datasets was performed. Thus, as studied before, it was used the $42 - 5 - 2$ ANN structure. As input, the datasets were composed by the resulting PSDs with bandpass filtering of frequencies [1, 30] Hz from the AF7 electrode position. The Tab. 6.7 displays the obtained accuracy results from the different subjects.

Table 6.7: Testing of different subjects using the resulting PSDs from the AF7 electrode position. The ANN structure used was $42 - 5 - 2$.

Subject	Test Accuracy (%)	Train Accuracy (%)
1	70,8	77,1
2	75,8	81,5
3	96,7	98,1

6.3 Results Discussion

As described in the State of the Art, one other study with the Muse headband for drowsiness detection, was conducted in 2017[35]. It was used the first version of the Muse headband and data from 23 subjects in both fresh and drowsy states. At first, they were able to obtain an accuracy of 81% with SVM and 76% with LDA, per subject. However, with cross-subject validation they obtained an accuracy of 74% with SVM and 68% with LDA. On the other hand, with a temporal aggregation strategy they were able to reach a cross-subject validation of 87%. Concerning the current project, as explained in chapter 5, it was used for the mind states classification a feed forward neural network. According to Tab. 6.7, the obtained results were: subject 1 - 70,8%, subject 2 - 75,8% and subject 3 - 96,7%.

Comparing both studies, similar accuracy was obtained using different approaches. The study from 2017 was able to reach a maximal accuracy of 87%, whereas the present study achieved a maximal of 96,7% in one of the subjects. However, the subjects accuracy average of the current study was 81,1%. Given that the maximal accuracy obtained in this work was considerably high, it shows that this approach can be successful.

Regarding the different accuracy results obtained from the different subjects, it can be due to diverse reasons. First, is the clairity of the difference between the alert and drowsy state. Perhaps, subject 3 was feeling more drowsy at the time of the recording in comparison to the other two subjects. Another really strong reason is the age factor. The recording from the oldest subject (subject 1) reached the lowest accuracy. As mentioned before, with age the subject alert state tends to not be as pronnounced. The alpha waves tends do decrease and theta waves may increase. Thus, the difference between the two mind states is not as clear. Concerning the subject 2, it was one of the persons responsable for conducting this study. Therefore, once for example in a drowsy state, the subject may become alert while thinking and worrying about the results. One other reason can be the remaining recording

artifacts and their influence in the obtained results.

Thus, for a more in dept study in the matter, more subjects should be tested. A larger number of datasets will better support this approach veracity. One factor that must be taken into consideration is the age. Hence, it's important to capture different EEG from subjects with different ages.

,

7

Conclusion

The main goal of the present project was to detect drowsiness, using brain waves read by a wearable and wireless EEG device, the MUSE brain sensing headset. The purpose was to test if a simple headband with a small number of electrodes could achieve results similar to the clinical grade devices.

From the analysis of the raw EEG signal, it was already possible to notice a higher influence of the artifacts in comparison with more complex EEG equipments. The Muse headband does a poor job on isolating the real EEG signal from the eye movements, muscle activity, surrounding noise and noise from other electronic devices. Thus, the sensitivity of Muse to noise represents a considerable disadvantage, since this device is meant to be used while driving, for example.

Concerning resolution, recordings from the Muse headband offer low resolution. There are various skull types, thus even though the headband is adjustable, it is hard to place the electrodes on the exact intended spot. Also, skin conditions will influence the signal quality. Another reason for the lack of resolution is the low number of electrodes and their position. On Chapter 2, it was mentioned that alpha frequencies, highly correlated with relaxation, are maximal on the occipital area. However, the Muse headset doesn't possess electrodes on this area. Concerning the theta waves, strongly associated with drowsiness, they are mostly present on the temporal lobe. Yet, the back electrodes of the Muse headband, on the temporal-parietal positions, are made with silicone-rubber which is more susceptible to artifacts, as described in the previous chapter. One other reason for the large number of artifacts amount is that the headband can easily move and loose contact with the skin.

After artifacts removal and processing of the EEG signal, the power spectral densities of both alert and drowsy states were analysed. With the Welch's method application it was possible to obtain the absolute powers from each brain wave. From the examination of the absolute powers it was possible to notice the lack of resolution of some recordings. Thus, the absolute powers weren't directly used for

the identification of drowsiness. However, they were important for calculating the relative powers.

With the examination of the relative powers from each mind state of each subject, it was possible to notice that lower frequency waves were more predominant on the drowsy state. On the other hand, higher frequency waves were more present on the alert state as expected. Regarding the alpha frequencies, different results were obtained. Subject 1 (49 years old) presented a higher amount of alpha waves on the drowsy state, whereas subjects 2 and 3 (both 23 years old) presented in the alert state. One reason for this result is the age factor and its correlation with the slowing of alpha waves in older subjects, as explained in Chapter 2.

As stated in Chapter 2, the theta band is highly related to the drowsy state. Thus, the ratio between the theta and alpha brain waves was calculated. As expected it was possible to observe a higher ratio on the drowsy state in all subjects.

With the purpose of exploring the machine learning area and the possibility of using the techniques for further work, the classification of both mind states with an ANN model was tested. After studying which would be the best input features and ANN structure, different accuracy results were obtained for each subject. The test accuracy results obtained were: subject 1 - 70,8%, subject 2 - 75,8% and subject 3 - 96,7%. Perhaps, one of the reasons for the lowest accuracy result could be also because of the age of the subject. The discrepancies between each mind state weren't much pronounced in this case.

In the future, to improve the obtained results, it is important to perform more recordings with different subjects and collect more datasets. As observed, each subject may present different results and therefore different conclusions. In the field of pre-processing of data, as described in Chapter 3, another technique that could be tested is ICA for artifact removal. One main disadvantage of the Muse headband is the large amount of different methods on this step should be tested. With more and larger datasets the ANN method should be better explored.

An interessant matter to be explored in further studies would be the influence of light, caffeine or sound while the subject is drowsy.

Bibliography

[1] Chin-Teng Lin, Yu-Chieh Chen, Ruei-Cheng Wu, Sheng-Fu Liang, and Teng-Yi Huang. Assessment of Driver's Driving Performance and Alertness Using EEG-based Fuzzy Neural Networks. 2005.

[2] Nicolas-Alonso Luis Fernando and Gomez-Gil Jaime. Brain Computer Interfaces, a Review. page 12(2): 1211–1279, 2012.

[3] Christos Papadelis, Chrysoula Kourtidou-Papadeli, Panagiotis D. Bamidis, Ioanna Chouvarda, D. Koufogiannis, E. Bekiaris, and Nikos Maglaveras. Indicators of Sleepiness in an ambulatory EEG study of night driving. 2006.

[4] M. Teplan. Fundamentals of EEG Measurement. *Measurement Science Reviwe*, 2, 2002.

[5] A. Casson, D. Yates, S. Smith, J. Duncan, and E. Rodriguez-Villegas. Wearable Electroencephalography. *IEEE Engineering in Medicine and Biology Magazine*, 29:44 – 56, 2010.

[6] Pouya Bashivan, Irina Rish, and Steve Heisig. Mental State Recognition via Wearable EEG. 2016.

[7] Fabrizio Sebastiani. Machine learning in automated text categorization. *Journal ACM Computing Surveys (CSUR)*, 34:1 – 47, 2002.

[8] Shih Jerry J., Krusienski Dean J., and Wolpaw Jonathan R. Brain-Computer Interfaces in Medicine. 87:268–279, 2012.

[9] T. M. Vaughan. Guest Editorial Brain-Computer Interface Technology: A Review of the Second International Meeting. *IEEE Transactions on Neural Systems and Rehabilitation Engineering*, 11:94–109, 2003.

[10] Niels Birbaumer. Breaking the silence: Brain–computer interfaces (BCI) for communication and motor control. *Psychophysiology*, 43, 2006.

[11] Xiao Jiang, Gui-Bin Bian, and Zean Tian. Removal of Artifacts from EEG Signals: A Review. 19, 2019.

[12] Nelly Elsayed, Zaghloul Saad Zaghloul, and Magdy Bayoumi. Brain Computer Interface: EEG Signal Preprocessing Issues and Solutions. *International Journal of Computer Applications*, 169, 2017.

[13] Angela T. Chan, Juan C. Quiroz, Sergiu Dascalu, and Jr. Frederick C. Harris. An Overview of Brain Computer Interfaces. 2015.

[14] Chang-Hee Han, Yong-Wook Kim, Do Yeon Kim, Seung Hyun Kim, Zoran Nenadic, and Chang-Hwan Im. Electroencephalography-based endogenous brain–computer interface for online communication with a completely locked-in patient. *Journal of NeuroEngineering and Rehabilitationvolume*, 16, 2019.

[15] Buxton RB, Uludağ K, and Liu TT Dubowitz DJ. Modeling the hemodynamic response to brain activation. *Neuroimage*, 23:S220 – S233, 2004.

[16] Seeck Margitta, Koessler Laurent, Bast Thomas, Leijten Frans, Michel Christoph, Baumgartner Christoph, He Bin, and Beniczky Sándor. The standardized EEG electrode array of the IFCN, Clinical Neurophysiology. (128):2070–2077, 2017.

[17] Trans Cranial Technologies ldt. 10/20 System Positioing Manual. 2012.

[18] Lim Seng Hooi, Humaira Nisar, Kang Wei Thee, and Vooi Voon Yap. A novel method for tracking and analysis of EEG activation across brain lobes. *Biomedical Signal Processing and Control*, (40):488 – 504, 2018.

[19] Kinaan Javed and Forshing Lui. Neuroanatomy, Cerebral Cortex. 2019.

[20] M.E. Goldberg. Parietal Lobe. *International Encyclopedia of the Social & Behavioral Sciences*, pages 11051 – 11054, 2001.

[21] Cassius Vinicius C. Reis, Kaan Yagmurlu, Ali M. Elhadi, Alexander Dru, Ting Lei, Sebastião N. S. Gusmão, Uédson Tazinaffo, Joseph M. Zabramski, Robert F. Spetzler, and Mark C. Preul. The Anterolateral Limit of the Occipital Lobe: An Anatomical and Imaging Study. *Journal Of Neurological Surgery*, 77:491 – 498, 2016.

[22] J Satheesh Kumar and P Bhuvaneswari. Analysis of Electroencephalography (EEG) Signals and Its Categorization - A Study. *Procedia Engineering*, (38):2525 – 2536, 2012.

[23] Soutar Richard. An Introductory Perspective on the Emerging Application of qEEG in Neuroffedback - Chapter 2, Clinical Neurotherapy. pages 19–54, 2014.

[24] Mahtab Roohi-Azizi, Leila Azimi, Soomaayeh Heysieattalab, and Meysam Aamidfar. Changes of the brain's bioelectrical activity in cognition, consciousness, and some mental disorders. *Medical Journal of the Islamic Republic of Iran*, pages 31 – 53, 2017.

[25] Mejdi Ben Dkhil, Ali Wali, and Adel M. Alimi. Drowsy Driver Detection by EEG Analysis Using Fast Fourier Transform.

[26] Juri D. Kropotov. Chapter 2.3 - Beta and Gamma Rhythms. *Functional Neuromarkers for Psychiatry - Applications for Diagnosis and Treatment*, pages 107 – 119, 2016.

[27] Juri D. Kropotov. Chapter 3 - Beta Rhythms. *Quantative EEG, Event-Related Potentials and Neurotherapy*, pages 59 – 76, 2009.

[28] H. Ueno, M. Kaneda, and M. Tsukino. Development of drowsiness detection system. 1994.

[29] S. Boverie, Giralt, J.M. Lequellec, and A. Hirl. Intelligent System for Video Monitoring of Vehicle Cockpit. 1998.

[30] Aleksandra Vuckovic, Vlada Radivojevic, Andrew C.N. Chen, and Dejan Popovic. Automatic recognition of alertness and drowsiness from EEG by an artificial neural network. 2002.

[31] Abdulhamit Subasi. Automatic recognition of alertness level from EEG by using neural network and wavelet coefficients. 2005.

[32] Hisashi Yoshida, Haruka Kuramoto, Yusuke Sunada, and Sho Kikkawa. EEG Analysis in Wakefulness Maintenance State against Sleepiness by Instantaneous Equivalent Bandwidths. 2007.

[33] Zahra Mardi, Seyedeh Naghmeh, Miri Ashtiani, and Mohammad Mikaili. EEG-based Drowsiness Detection for Safe Driving Using Chaotic Features and Statistical Tests.

[34] Timothy Brown, Robin Johnson, and Gary Milavetz. Identifying Periods of Drowsy Driving Using EEG. 2013.

[35] Fnu Rohit, Vinod Kulathumani, Rahul Kavi, Ibrahim Elwarfalli, Vlad Kecojevic, and Ashish Nimbarte. Real-time drowsiness detection using wearable,

lightweight brain sensing headbands. *IET Intelligetn Transport Systems*, 11:255 – 263, 2017.

[36] Zartashia Shameen, Mohd Zuki Yusoff, Mohamad Naufal Mohamad Saad, Aamir Saeed Malik, and Muhammad Muzammel. Electroencephalography (EEG) Based Drowsiness Detection For Drivers: A Review. 2018.

[37] Gang Li and Wan-Young Chung. A Context-Aware EEG Headset System for Early Detection of Driver Drowsiness. 2015.

[38] Nadia Mammone, Fabio La Foresta, and Francesco Carlo Morabito. Automatic Artifact Rejection From Multichannel Scalp EEG by Wavelet ICA. 12, 2012.

[39] KOVACEVIC Natasha, RITTER Petra, TAYS William, MORENO Sylvain, and MCINTOSH Anthony Randal. 'My Virtual Dream': Collective Neurofeedback in an Immersive Art Environment. 2015.

[40] Li Tan and Jean Jiang. Digital Signal Processing (Second Edition). pages 555 – 619, 2013.

[41] Shayan Motamedi-Fakhr, Mohamed Moshrefi-Torbati, Martyn Hill, Catherine M. Hill, and Paul R. White. Signal processing techniques applied to human sleep EEG signals—A review. *Biomedical Signal Processing and Control*, 10:21 – 33, 2016.

[42] Lindsay Brown, Jef van de Molengraft, Refet Firat Yazicioglu, Tom Torfs, Julien Penders, and Chris Van Hoof. A low-power, wireless, 8-channel EEG monitoring headset. 2010.

[43] Matti Siekkinen, Markus Hiienari, Jukka K. Nurminem, and Johanna Nieminen. How Low Energy is Bluetooth Low Energy? Comparative Measurements with ZigBee/802.15.4. *WCNC 2012 Workshop on Internet of Things Enabling Technologies, Embracing Machine-to-Machine Communications and Beyond*, pages 232 – 237, 2012.

[44] Aleksandra Przegalinska, Leon Ciechanowski, Mikolaj Magnuski, and Peter Gloor. Muse Headband: Measuring Tool or a Collaborative Gadget? 2017.

[45] A. S. Baran, C. Koen, and B. Pokrzywka. A detection threshold in the amplitude spectra calculated from *Kepler* data obtained during K2 mission. *Monthly Notices of the Royal Astronomical Society*, 448:L16 – L19, 2015.

[46] Ke Wu, Lei Zhu, and Ruediger Vahldiech. The Electrical Engineering Handbook. pages 585 – 618, 2005.

[47] George Ellis. Control System Design Guide (Fourth Edition). pages 165 – 183, 2012.

[48] W. T. Cochran, J. W. Cooley, D. L. Favin, H. D. Helms, R. A. Kaenel, W. W. Lang, G. C. Maling, D. E. Nelson, C. M. Rader, and P. D. Welch. What is the fast Fourier transform? *Proceedings of the IEEE*, 55:1664 – 1674, 1967.

[49] K.R. Rao, Do Nyeon Kim, and Jae Jeong Hwang. Fast Fourier Transform - Algorithms and Applications. 2011.

[50] G. D. Bergland. A guided tour of the fast Fourier transform. *IEEE Spectrum*, 6:41 – 52, 1969.

[51] Rainer Martin. Noise Power Spectral Density Estimation Based on Optimal Smoothing and Minimum Statistics. *IEEE Transactions On Speech And Audio Processing*, 9(5):504 – 512, 2001.

[52] Eric McAdams. Bioelectrodes. *Encyclopedia of Medical Devices and Instrumentation*, 2006.